PARAMETRIC STUDY OF A DIRECT CARBON SOLID OXIDE FUEL CELL THAT UTILIZES GASIFICATION FOR EFFICIENT ENERGY PRODUCTION AND MANUFACTURE OF A PROTOTYPE TO PROVIDE PROOF OF CONCEPT

A Final Year Project Progress Report

Presented to

SCHOOL OF MECHANICAL & MANUFACTURING ENGINEERING

Department of Mechanical Engineering

NUST

ISLAMABAD, PAKISTAN

In Partial Fulfillment

of the Requirements for the Degree of

Bachelors of Mechanical Engineering

---

by

Ahmed Wahaj

Haris Shahzad

Zain ul Abideen

June, 2018

EXAMINATION COMMITTEE

We hereby recommend that the final year project report prepared under our supervision by:

AHMED WAHAJ	NUST201433395BSMME11114F.
HARIS SHAHZAD	NUST201433663BSMME11114F.
ZAIN UL ABIDEEN	NUST201432539BSMME11114F.

Titled: "PARAMETRIC STUDY OF A DIRECT CARBON SOLID OXIDE FUEL CELL THAT UTILIZES GASIFICATION FOR EFFICIENT ENERGY PRODUCTION AND MANUFACTURE OF A PROTOTYPE TO PROVIDE PROOF OF CONCEPT" be accepted in partial fulfillment of the requirements for the award of BE MECHANICAL degree with grade __.

Supervisor: Dr. Emaddudin, Assistant Professor Supervisor	Dated:
Committee Member: Dr Zaib Ali Assistant Professor Advisor	Dated:
Committee Member: Sir Shoaib Ahmed Lecturer Advisor	Dated:

_____ _____

(Head of Department) (Date)

COUNTERSIGNED

Dated: _____ _____

(Dean / Principal)

ABSTRACT

The energy demand of Pakistan is steadily increasing and so is the gap between energy supply and demand. There has been a shift towards renewable sources of energy in some parts of the world, particularly Europe. Pakistan, however, continues to rely on fossil fuels to generate electricity. The advent of fuel cells has allowed us to more efficiently extract energy from fossil fuels. Fuel cells can be more than twice as efficient as their combustion counterparts.

With our aim to work towards a sustainable future for Pakistan and for humanity, we aim to accelerate the introduction of fuel cells into the energy mix of Pakistan by designing a solid oxide direct carbon fuel cell that will be able to convert the chemical energy of coal into electrical energy by incorporating a gasifier into our design.

Our project involves a parametric design of the fuel cell, encompassing all critical elements of a fuel cell from the material of the electrodes to the ideal fuel and the gasifier conditions. By simulating the entire model of the fuel cell, we wish to optimize its performance parameters such as the current density and the power density and finally by developing a prototype single stack fuel cell, wish to highlight its importance towards creating a feasible future for humanity.

ACKNOWLEDGEMENTS

A lot of hard work and guidance was required for this projects completion. We are all very thankful to the people that went out of their way to help us in our project.

We thank our supervisor, Assistant Professor Dr Emad and our Advisors, Dr Zaib and Sir Sohaib for the constant guidance they have provided us and providing us with the opportunity to work with them.

ORIGINALITY REPORT

Originality Report

ORIGINALITY REPORT

11%	4%	8%	4%
SIMILARITY INDEX	INTERNET SOURCES	PUBLICATIONS	STUDENT PAPERS

PRIMARY SOURCES

1	Lin, C.K.. "Thermal stress analysis of a planar SOFC stack", Journal of Power Sources, 20070110 Publication	3%
2	Submitted to University of Newcastle upon Tyne Student Paper	1%
3	Submitted to University of Birmingham Student Paper	1%
4	O'Hayre, Ryan, Suk-Won Cha, Whitney Colella, and Fritz B. Prinz. "Chapter 2: Fuel Cell Thermodynamics", Fuel Cell Fundamentals, 2016. Publication	1%
5	etd.lib.metu.edu.tr Internet Source	1%
6	Submitted to Indian Institute of Science, Bangalore Student Paper	<1%

Exclude bibliography Off

AP Dr. Emad ud Din

TABLE OF CONTENTS

LIST OF TABLES

LIST OF FIGURES

ABBREVIATIONS

PEMFC	Polymer Electrolyte Fuel Cell
AFC	Alkaline Fuel Cell
PAFC	Phosphorus Acid Fuel Cell
MCFC	Molten Carbonate Fuel Cell
SOFC	Solid Ocide Fuel Cell
K.E	Kinetic Energy
P.E	Potential Energy

NOMENCLATURE

j_{0a}	anodic exchange current density
j_{0c}	cathodic exchange current density
$\vec{J}_i$	diffusive mass flux of species i
k_e	electrolyte thermal conductivity
k_{elec}	thermal conductivity of electrode, anode or cathode thermal conductivity.
k_{int}	thermal conductivity
k^{eff}	effective thermal conductivity
n	number of electrons participating in the reaction
N_j	molar fluxes of other species, from j to n (except *i*)
$\vec{N}_i$	molar flux density of species *i*
p	fluid pressure
P	partial pressure
P_{gas}	reactant gas pressure
P_i	partial pressure of species i
P^0	standard gas pressure
R	gas constant (8.314472 $JK^{-1}mol^{-1}$)
R_{ct}	intrinsic charge transfer resistance
R_{elec}	electrode electrical resistance, anode or cathode electrical resistance.
S_e	energy due to a source term
S_{el}	source term calculated from the reactions
S_{io}	source term calculated from the reactions

S_m	additional mass sources
S_{rad}	energy due to a radiation term
$S_{s,i}$	additional species sources
$\vec{S}_M$	external body force
T	reaction temperature
T_{fur}	furnace inner surface temperature
T_{int}	SOFC outer surface temperature
V	velocity vector
V	actual cell voltage
V_{oc}	open circuit voltage
V_v	fractional porosity
W	width and length of unit cell
X_i	concentration of species i
X_j	concentration of other species, from j to n (ex- cept i)
z	number of electrons participating in the electro- chemical reaction
Δx	length of unit cell
α_1	Thermal Expansion coefficient of first layer
α_2	Thermal Expansion coefficient of second layer
α_3	Thermal Expansion coefficient of third layer
t_1	Thickness of first layer
t_2	Thickness of second layer
t_3	Thickness of third layer

η Thickness of joint between first and second layer

η' Thickness of joint between second and third layer

G Shear modulus of joint between first and second layer

G' Shear modulus of joint between second and third layer

F_1 Shear force on first layer

F_2 Shear force on second layer

F_3 Shear force on third layer

T Thermal loading temperature

T_0 Initial temperature

τ Shear stress in first bonded joint

τ' Shear Stress in second bonded joint

Greek letters

α_a charge transfer coefficients of anodic reactions

α_c charge transfer coefficients of cathodic reac- tions

α_i charge transfer coefficients of substances where *i* represents each species in the reactions

η polarization

η_{act} activation polarization

η_{conc} concentration polarization

η_{ohm} ohmic polarization

v_i stoichiometric coefficients where i represents each species in the reactions

ρ fluid density

$\vec{\tau}$ stress tensor

μ fluid viscosity

ε porosity

ζ shear stress tensor of the fluid

κ permeability

σ_i ionic conductivity of electrode

σ_{io}^{eff} conductivity of the purely ionic conducting material

σ_{el}^{eff} conductivity of the purely electronic conducting material

$\emptyset_{io}$ ionic potential

$\emptyset_{el}$ electronic potential

CHAPTER 01 – INTRODUCTION

1.1 PROBLEM IDENTIFICATION

Growing up in a country facing a severe energy shortfall and where blackouts lasting 8-10 hours a day are the norm instead of anomalies, we have always been acutely aware of need to work towards a sustainable future for humanity. With the fossil fuel reserves running out, it is the need of the hour to work on alternative forms of energy while also utilizing our existing fossil fuels in an efficient manner.

1.2 MOTIVATION

Renewable energy is, without a doubt, the need of the hour and the transition towards wind, solar and other renewable sources is a necessity. However, the switch will be a long and tedious process. Solar energy in particular is plagued by the fact that it is extremely intermittent and can only be used where there is sufficient energy. The variation in power of the solar cells throughout the day is also a cause of concern. It is also relatively costly and an inefficient process. Although, research into improving the materials of photovoltaic cells is ongoing in an effort to improve their efficiency, it is definitely a long way before energy can be harvested from them in an efficient manner.

Wind energy is a very viable alternate and have become, overtime, extremely efficient in converting the kinetic energy of the wind to electrical energy. The current efficiency of wind turbines is very close to the Betz limit or the maximum possible efficiency that can be achieved by utilizing the power of wind. It can be installed, however, only in places where there is a steady supply of wind. Also, to harvest sufficient energy, it is important to make the wind turbines sufficiently high because the speed of wind is greater as you go higher. This poses a risk to birds who often suffer casualties as they collide with the blades of the wind turbine. For wind to be considered a viable alternative to fossil fuels, it must find ways to overcome the apparent problems that hinder its use.

Even if breakthroughs via research were to make the use of solar and wind energy extremely efficient, cheap and viable in the coming years, there are still many other problems that need to be addressed. The fact that they can only be installed in select areas

(areas of high sunshine for solar energy and regions of steady wind for wind energy) means that they must often be installed far away from where the energy is required. The further away they are, the more the line losses that we will have to bear in order to transport the energy from where it is being generated to where it is needed. These line losses will make the process overall extremely inefficient.

The inherent intermittent nature of solar and the unpredictable nature of wind energy means that it is necessary to store energy for times when it may not be available. Lithium Ion batteries have been dramatically improved in recent years but their power density is still extremely low as compared to a fuel such as oil.

Most of the energy being produced in Pakistan is via fossil fuels and there has been an increased use of coal in recent years. Wind energy projects have been initiated in Sindh, particularly in the Jhimpir and Thatta areas and there is also a mega solar project underway. However, they would still contribute little to the energy mix of Pakistan once commissioned.

The population of Pakistan continues to grow and brings with it a higher energy demand. The current shortfall will continue to increase until steps are taken to improve the situation. The abundance of coal, albeit that of low quality, means that it is a viable option to address the energy needs of Pakistan.

It is no secret that coal power plants are plagued with their own problems. Although the energy that they produce is not intermittent because the power plant can run almost throughout the year, 24 hours a day, with very little downtime, it also contributes to global warming and results in the release of toxic gases to the environment. The sulfur content contained within coal give rise to dangerous oxides of sulfur that contribute to pollution. On top of all that, the combustion of coal is a very inefficient process that is only able to utilize about 30% of the available energy.

Fuel cells offer a very attractive alternative to coal power plants. Fuel cells have a much higher efficiency in the range of 70-80%, much higher than that of a coal power plant. A careful design may also help ensure that the sulfur oxides that are emitted during the operation of a coal power plant, are eliminated. Fuel cells offer high power densities so we

can extract a sufficient amount of energy from a small area. Power densities in the range of 4000-5000 Watts per meter square are not uncommon.

Furthermore, investing in fuel cell research is investing in the future because fuel cells can not only be used to harvest energy from coal, but also from methane and hydrogen. Hydrogen is a zero-carbon emission fuel and possibly the future of producing energy because of the high amount of energy it produces per kilogram of fuel. Hydrogen as a fuel is being very seriously researched upon and the different methods of producing it, including solar catalysis of water, are steadily gaining increased popularity. The method of harvesting energy from hydrogen fuel are fuel cells.

So, fuel cells are not only a viable option of using our current resources in an efficient manner but also a way by which we could work on alternative, cleaner sources of energy.

A sad reality is that there is very little research ongoing in Pakistan right now related to the use of fuel cells for producing energy. While people all around the world are trying to bring commercial fuel cell stacks into the market, the people of Pakistan are blissfully ignorant of its inherent advantages.

Our motivation, therefore, was to develop a prototype for a fuel cell that would allow us to promote research towards the topic and also make people aware of how it is a solution to the energy problems that are plaguing Pakistan. The project would allow us to work on a meaningful project that would allow us to help benefit Pakistan and humanity as a whole.

1.3 AIM:

"Development of a fuel cell prototype that effectively uses local carbon reserves"

1.4 OBJECTIVES

- Selection of a Fuel Cell type
- Selection of Fuel.
- Selection of Materials.
- Numerical Analysis and design of a gasifier to produces Syngas (Carbon Monoxide) using Reverse Boudouard Reaction.
- Parametric Analysis, design and manufacturing of a fuel cell that utilizes carbon to produce energy.

CHAPTER 02 – LITERATURE REVIEW

Coal is a major source of producing energy throughout the world. It is a main resource in production of electricity. Around 40% of the electricity in the world is generated using coal.1 [9] Right at this very moment in terms of generating world's primary energy it is the second biggest resource, and it is widely anticipated that it will occupy oil's position on the top of the list of the largest sources of globe's primary energy.[9] As per BP Statistical Review of World Energy 2016, 891,531 million tonnes of reserves of coal were reported on a global level.[10] If we keep the yearly utilization of coal in mind, it can be safely predicted that even by the end of year 2112, coal will still be present for use, and by the end of 2042, it will be the only source of primary energy left in the world. [11]

Many nations and countries in the world have huge coal reserves and Pakistan is one of them. Approximately 186 billion tonnes of coal reserves are present in Pakistan, which is much more than the estimated gas and oil reserves in Pakistan. [12]At present, coal power plants are consuming the coal present in Pakistan. At a global level, on average the efficiency of coal power plants is merely 33%. [13]

Carbon fuel cell is a more feasible and beneficial option for utilization of coal as compared to coal power plants. Unique in its nature, this cell operates at high temperature which involves the utilization of fuel and carbon as anode. It generates electricity and compared to coal-fired power plants it is much more efficient. Also, in comparison to coal power plants, the rate and quantity of emissions is very low. [14]The direct carbon fuel cell utilizes electrochemical oxidation to produce electrical power from the chemical energy of the carbon available. Fuel usage is around 100% because the fuel and the gases produced are in unique phases which makes their separation and utilization extremely easy. As far as other cells are concerned, the same cannot be done and thus the efficiency of fuel usage is reduced to around 85%. Also, 100% is the approximated theoretical efficiency. These two important reasons, result in around 80% the efficiency of electrical power production through direct carbon fuel cell – which is two times the efficiency of the average coal-fired power plant, and also resulting in half the emissions of green-house gases as compared to power plants. [15]Quantity of carbon dioxide produced is also around 50% of the quantity produced through coal power plants. Additionally, the produced gas is around 100% carbon

dioxide, resulting in almost negligible requirement of gas separation prior to sequestration. Thus, in comparison to other advanced methods, there will be less energy and financial expenditures to separate and store carbon dioxide. Moreover, different fuels in large

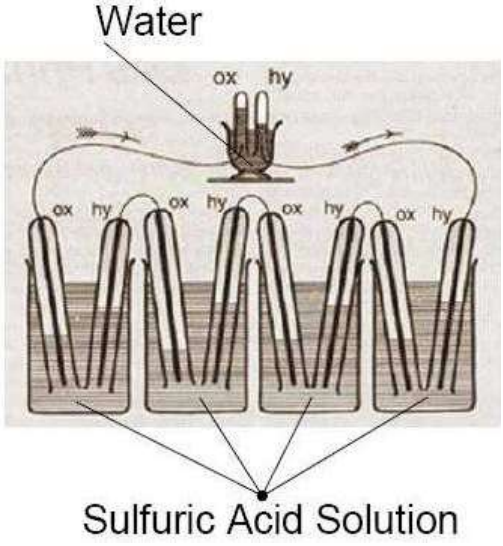

Figure 1: A diagram of Grove's gas voltaic cell.

quantities e.g. organic waste, coal, biomass, coke and tar may be utilized, as well.

Even though they were not known by most people, initial developments in fuel cells started during 1800s. Sir Humphry Davy during 1801, present the idea of fuel cell. He was the first to do so. Christian Friedrich Schonbein got accreditation during 1838 for developing the first fuel cell. Sir William Robert Grove, belonging from Wales was a judge and a scientist who had immense expertise in researching fuel cells. During 1839 he invented the 'gas battery' presently called the 'Grove cell'. William Robert Grove proved that when hydrogen and oxygen are made to react electrochemically, electrical power is generated. Figure 1 is the fuel cell that William Robert invented. After many months, during 1840, William Robert presented first incandescent light. Thomas Edison improved upon this idea. Ludwing Mond and Charles Langer also utilized and worked on the concept of 'Gas Battery'. During 1889, this refinement and advancement was given the name 'fuel cell'. In 1950s, many actual and important advantages of fuel cells could be seen after many advancements. During 1959 5 kW fuel cell system was developed through manipulation of the concept of the Langer and Mond cell by Francis Thomas Bacon. In the same year, Harry Karl Ihrig further manipulated 5 kW system developed by Bacon resulting in a 15 kW cell

stack which was utilized to run a tractor. The organization behind the act of utilization of the fuel cell to run the tractor, started utilization of fuel cells to run the US Air Force vehicles and submarines.

Subsequent to developments of Bacon and Ihrig, in various high-scale projects, fuel cells played a massive role. During 1960s, NASA utilized the fuel cells as fuel cell generators on its space program. Gemini space program again utilized these fuel cell generators halfway through the decade. Apollo space missions also utilized the fuel cells to generate electricity and provide drinkable water to astronauts embarked on space campaigns. Because of such campaigns, on all space missions, these cells were utilized. Soviet Union also worked on fuel cells for utilization in submarines and space programs.

In 1970s, fuel cells received major advancements, government legislations on emissions from transport and concerns related to environment grew drastically. General Motors (GM) demonstrated, for the first time, the concept of fuel cell electric transport. Towards the start of 20th Century, most of the great car manufacturing organizations began to give attention to the concept of fuel cells in some way. But, fuel cars became commercial and could be accessed by people during 2008.

In 1990s, government began to fund development and research in fuel cells because solid oxide fuel cells and polymer electrolyte fuel cells gained importance as stationary and portable sources of electricity. Significantly, in the field of combined heat and power (CHP) units where the thermal energy and electricity is used in micro-generation points. A mandate was presented in California, in the 1990s whose aim was to come up with other ways to power vehicles; this gave a great boost for zero emissions transportation. This era is also a witness to the early utilization of fuel cells in mobile devices such as mobile phones and laptops even though the portability of this equipment was not compared to those powered by a standard battery. [16]

There are many uses of fuel cells and also for every particular use, there is a specific fuel cell. The uses of fuel cells are of 3 major types: *portable, transportation and stationary power* [17]

Portable uses of fuel cells contain those that are fitted in, or provide charge to, that can be carried around by the user for generating power.[17] Many types of portable devices can utilize the power range of 5W – 500kW within this specific area of usage. Few utilities of

fuel cells in portable power devices are personal computers, cellphones, hearing aids (fuel cell recharges the battery of hearing aid) and in military equipment. Within this area of application, to substitute or play a supportive role for the present power systems, direct methanol fuel cells and polymer electrolyte membrane fuel cells are used. The advantage of fuel cells in H_2 for polymer electrolyte membrane fuel cells and CH_3OH for direct methanol fuel cells despite being a less expensive and less heavy substitute for batteries but can also be carried around easily. [18]When they are used alongside the present battery-powered systems, they become a source of really quick charging. [17]

A major field where fuel cells can be utilized is the *transportation* sector. Fuel cells can be used as a substitute for the primary power source in vehicles. It can also be used in conjunction with the current battery stack system to extend the life and time of the battery-powered systems in present vehicles. The use of fuel cells is not simply restricted to cars on roads but they can also be used in auto driving applications in boats, trains and any other mode of transportation which utilizes the the IC engine or electrical one. But, the major focus on many great companies is to substitute the IC engines with the fuel cells battery hybrid systems. A list of vehicles operating on fuel cells is present in Fuel Cells (2003) which gives further detailed information on kinds of fuel cells and their ranges for specific vehicles depending upon the requirements and applications. Even though this is just a start and there is still some time in seeing the fuel cell powered vehicles on roads at a common level, car manufacturers have the goal to produce and sell such cars expectedly in 2015[17]. One of the drawbacks of fuel cell cars at a commercial level is that there is no proper infrastructure for the refueling and provision of pure H_2. Polymer electrolyte fuel membrane cells has been considered as the most optimum and suitable kind of fuel cell that should be utilized in the transportation sector. Even though the fuel cells are far more efficient that IC engines, the main reason why polymer electrolyte membrane fuel cells are considered the most suitable is because they operate at a low temperature due to which the startup time is very short, and thus suitable in scenarios where quick power is required by the person who wants to start driving their car as soon as they get in without having to wait out the starting time.

The idea of *stationary power* is that primarily electrical energy is generated along with some thermal energy by a stationary source. Presently, the sources of stationary power are the coal-fired power plants that produce electricity at their own specific locations and then

the electricity is distributed according to the requirements of specific areas within the country. A kind of boiler system is normally used to produce thermal energy for such sites. Combined heat and power systems are used to vary the way thermal energy is generated and supplied. to generate thermal energy and electrical power from fuel cell installed in a system similar to a boiler is the main purpose of CHP system. Such combined heat and power systems range from 0.5kWe and l0kWe. They have efficiency between 80-95% when both electricity and heat is used[17]. Combined heat and power system, though only affordable when government funds such systems, are being used extensively in East-Asian countries like South Korea and Japan. To fulfill the requirements of heat and electricity, fuel cells remain in operation almost continuously. This makes up for the rapid fire up time which was critical in other applications related to transportation. Hence, for this sort of application, polymer electrolyte membrane fuel cell, molten carbonate fuel cell and solid oxide fuel cells are majorly considered with solid oxide fuel cell being the most appropriate one for such applications. The most beneficial aspect of solid oxide fuel cell is that it can utilize natural gas as well which makes the introduction of SOFCs in the present infrastructure no problem at all from both cost and time scale perspective.

There are various kinds of fuel cells. Type of electrolyters, operation temperature and conducting ions that pass through the electrolyte are major factors for differentiating between and classifying different fuel cell types. Major types of Direct Carbon Fuel Cells (DCFC) exist as follows. 1.Polymer Electrolyte Membrane Fuel Cell (PEMFC) 2. Direct Methanol Fuel Cells 3. Alkaline Fuel Cell (AFC) 4. Phosphoric Acid Fuel Cells 5. Molten Carbonate Fuel Cells 6. Solid Oxide Fuel Cells (SOFC)

Table 1: Types of Fuel Cells [19]

Fuel cell	Abbreviation	Mobile ion	Operating Temperature
Polymer Electrolyte Fuel Cell	PEMFC	H^+	60-80°C
Alkaline Fuel Cell	AFC	OH^-	50-200°C
Phosphoric Acid Fuel Cell	PAFC	H^+	≈ 200°C
Molten Carbonate Fuel Cell	MCFC	CO_3^{-2}	≈ 650°C
Solid Oxide Fuel Cells	SOFC	O^{-2}	600-1000°C

Table 2 Fuel Impact on Various Fuel Cells [19]

Fuel	PEMFC	AFC	PAFC	MCFC	SOFC
H_2	fuel	fuel	fuel	fuel	fuel
CO	poison (50ppm per stack)	poison	poison ($< 0.5\%$)	fuel	fuel
CH_4	diluent	poison	diluent	diluent	fuel
CO_2 & H_2O	diluent	poison	diluent	diluent	diluent
S		poison	poison ($< 50ppm$)	poison ($< 0.5ppm$)	poison ($< 1ppm$)

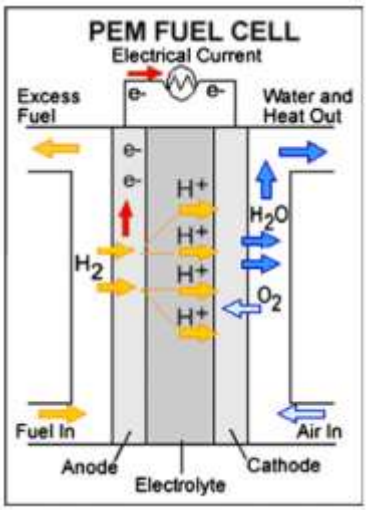

Figure 2: Schematic of a PEM fuel cell[6]

The *polymer electrolyte membrane fuel cell (PEMFC)* has other names lik proton exchange membrane fuel cell, polymer electrolyte fuel cell and solid polymer fuel cell. Polymer membrane which conducts ions is used as an electrolyte. On sides of the membrane, anode and cathode are bonded. Such arrangement has been generally named as membrane electrode assembly that can be placed between the flow field plates (bipolar plates) to make an assembly called "stack". Polymer electrolyte membrane fuel cell operates in a way similar to that of an acid electrolyte cell since the ions in the polymer are H+ or proton. [20]

At Anode:

$$H_2 \longrightarrow 2H^+ + 2e^-$$

At Cathode:

$$\frac{1}{2}O_2 + 2H^+ + 2e^- \longrightarrow H_2O$$

Overall Reaction:

$$H_2 + \frac{1}{2}O_2 \longrightarrow H_2O$$

PEMFCs are expensive and this is a major factor that restricts their vast applications in various fields. In 2009, a PEMFC was developed which cost around 61$ and its operation life was registered as 2500h when used in the field of transport. PEMFCs are better than internal combustions in many ways apart from the cost. [6]The drawback is the heat produced from PEMFC which cannot be effectively used in all applications. Another drawback of PEMFC is the need of platinum which is used to support the electrochemical reactions. PEMFC operates at a low temperature which means that the amount of heat produced by the PEMFC is very small for endothermic reformation. [20]

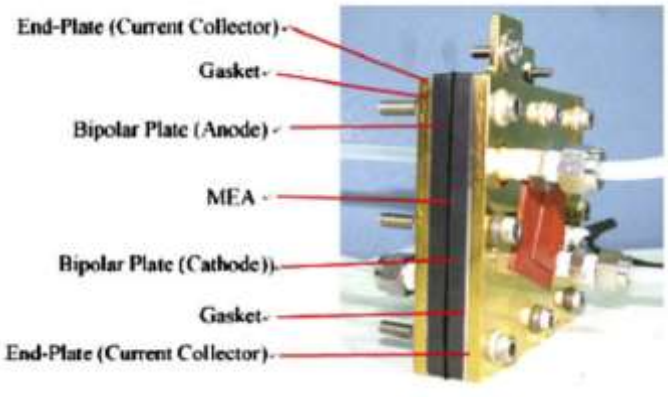

Figure 3: Basic components of a direct methanol fuel cell [3]

The *direct methanol fuel cell (DMFC)* is regarded as the optimum fuel cell system because it generates electricity by directly utilizing methanol at anode. This gives DMFC an edge over the generic fuel cells, especially in applications in transport, that depend on huge reforming assemblies to produce H_2 from methanol and similar hydrocarbons.

At Anode:

$$CH_3OH + H_2O \longrightarrow CO_2 + 6H^+ + 6e^-$$

At Cathode:

$$\frac{1}{2}O_2 + 6H^+ + 6e^- \longrightarrow 3H_2O$$

Overall Reaction:

$$CH_3OH + \frac{1}{2}O_2 \longrightarrow CO_2\ 3H_2O$$

The production of DM fuel cell at a commercial level has been limited because of its abysmal performance in comparison with air/hydrogen systems, greatly impeded by the performance of anode that demands most efficient of methanol oxidation catalysts. Research was conducted to find catalysts of this nature and it was found that only platinum-based substances show prominent activity and desired stability. [21]However, platinum-based substances and platinum itself is very costly and require a hefty initial expense. [22]

Alkaline Fuel Cells (AFCs) utilize aqueous KOH solution for electrolyte, at a concentration of around 30%. [23] The electrodes have a two-layer structure: an active electrocatalyst layer, and a hydrophobic layer. Utilization of non-noble metal electrocatysts is allowed by the inherently faster kinetics of redox reactions in an AFC. [4]

At Anode:

$$2H_2 + 4OH^- \longrightarrow 4H_2O + 4e^-$$

At Cathode:

$$O_2 + 2H_2O + 4e^- \longrightarrow 4OH^-$$

Overall Reaction:

$$2H_2 + O_2 \longrightarrow 2H_2O$$

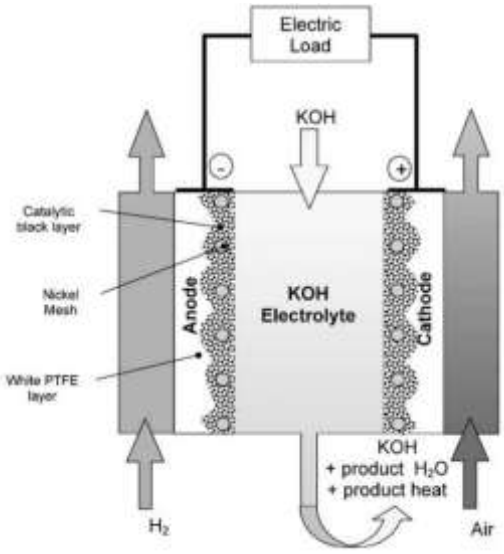

Figure 4: Alkaline Fuel Cell composition [4]

The production of CO_2 poisons the AFC and adversely effects its performance with time and as a result the generation of power from hydrocarbons is limited so some extent. [24]Just like other kinds of fuel cells, Alkaline Fuel Cells have a specific tolerance to the quantity of impure substances. Any harmful substances that include different gas like CO_2 can cause degradation of the fuel cell. In addition, to separate carbon dioxide from the stream of feed gases is not feasible because it results in hefty expenses. [4]

Phosphoric acid fuel cells (PAFC) utilize H_3PO_4 as an electrolyte in liquid form. The electrolyte consisting of phosphoric acid conducts protons due to which the protons simply travel to the cathode from the anode while an external circuit is required for the migration of electrons. At cathode, air is supplied. O_2 reacts with protons and electrons supplied by electrolyte and external load. [5]

At Anode:

$$H_2 \longrightarrow 2H^+ + 2e^-$$

At Cathode:

$$\frac{1}{2}O_2 + 2H^+ + 2e^- \longrightarrow H_2O$$

Overall Reaction:

$$H_2 + \frac{1}{2}O_2 \longrightarrow H_2O$$

Just like other fuel cells that do not operate at a high temperature, CO has adverse effects on the performance of PAFC. This is because the carbon monoxide causes degradation of the platinum catalyst. Platinum catalysts have high costs. Carbon and graphite are used to support the platinum catalyst. But, when carbon and graphite are utilized the performance of the fuel cell is somewhat restricted. Specifically, to prevent any sort of corrosion in the fuel cell, it is advised that the operation voltage be less than 0.8V. [25]At high voltages, Pt electrode is dissolved due to which there is no presence of any sort of metallic substance

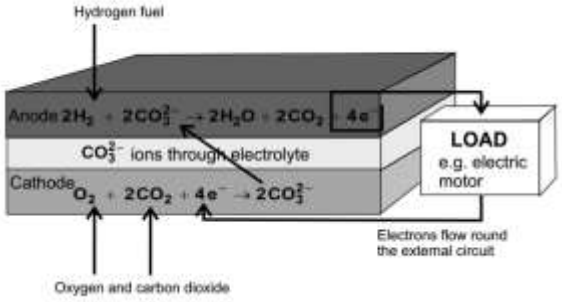

Figure 5: Phosphoric acid fuel cell schematic [5]

to catalyze the corrosion of carbon. Additionally, a drawback of using carbon with platinum is that platinum tends to migrate to the upper surface of carbon and cover, thereby lessening, the active surface area by lumping together in large quantity on the surface.

Just like the rest of the FCs, the operation of the *(Molten Carbonate Fuel Cell) MCFC* is relies on reaction of H_2 and O_2 resulting in H_2O via an electrolyte that carries electrons. For the anodic reaction, the H_2 supplied is produced from CH_4 in MCFC by a procedure called 'steam reforming'. CH_4, the constituent of natural gas that carries energy, reacts with H_2O to burn the carbon, thereby releasing all the H_2 from CH_4 and H_2O. This procedure utilizes the thermal energy from the FC. Subsequent to the removal of Sulphur and higher hydrocarbons, a direct feed of mixture of H_2O and CH_4 can be directed to the MCFC with

internal reforming — we call it the direct fuel cell (DFC). [26]

Internal Reformer:

$$CH_4 + H_2O \longrightarrow 3H_2 + CO$$

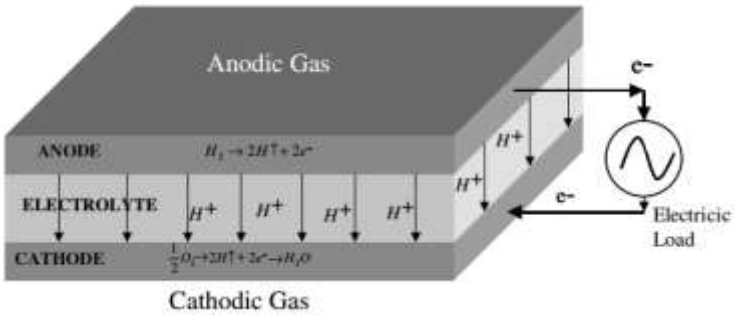

Figure 6: Operating prinicple of MCFC when hydrogen is used as fuel [2]

At Anode:

$$H_2 + {CO_3}^{2-} \longrightarrow H_2O + CO_2 + 2e^-$$

At Cathode:

$$\frac{1}{2}O_2 + CO_2 + 2e^- \longrightarrow {CO_3}^{2-}$$

Overall Reaction:

$$H_2 + \frac{1}{2}O_2 \longrightarrow H_2O$$

The cathode is made of lithiated NiO which is a major drawback in molten carbonate fuel cell because it can dissolve easily. The NiO material after dissolution in electrolyte undergoes transportation, reduction and precipitation in the electrolyte matrix. [27]

The *solid oxide fuel cell (SOFC)* also known as ceramic fuel cell has a distinguishable characteristic that it has a metallic oxide, solid ceramic electrolyte. The typical assembly of a planar solid oxide fuel cell it consists of anode, cathode, electrolyte, interconnect plates and sealing material. [28]Practically, if more than one cell has to be utilized, they are

'stacked' together. At the negative electrode, reduction of O_2 to O^{2-} takes place, which then are transported to the positive electrode via electrolyte where they undergo a reaction with the fuel, normally H_2 and CO, producing H_2O and carbon dioxide, along with electrical power and thermal energy.

The hydrocarbon fuel is reacted in the presence of a catalyst, normally to produce synthesis gas also known as syngas ($CO+H_2$), in the solid oxide fuel cell itself. Carbon monoxide and hydrogen undergo electrochemical oxidation to produce CO_2 and H_2O at positive electrode, along with electricity and thermal energy.

At Anode:

$$H_2 + O^{2-} \longrightarrow H_2O + 2e^-$$

$$CO + O^{2-} \longrightarrow CO_2 + 2e^-$$

At Cathode:

$$O_2 + 4e^- \longrightarrow 2O^{2-}$$

Overall Reaction:

$$H_2 + CO + O_2 \longrightarrow H_2O + CO_2$$

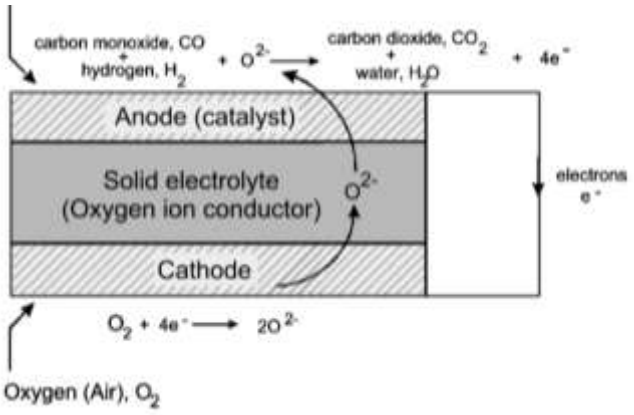

Figure 7: Schematic of SOFC [1]

Table 3 Reactions at Anode of an SOFC [7, 8]

Reaction	Equation
Methane steam reforming	$CH_4 + H_2O \rightarrow 3H_2 + CO$
Methane dry reforming	$CH_4 + CO_2 \rightarrow 2H_2 + 2CO$
Shift reaction	$CO + H_2O \rightarrow H_2 + CO_2$
Methane full combustion	$CH_4 + 2O_2 \rightarrow 2H_2O + CO_2$
Methane partial oxidation	$CH_4 + \frac{1}{2}O_2 \rightarrow 2H_2 + CO$
Hydrogen full combustion	$H_2 + \frac{1}{2}O_2 \rightarrow H_2O$
Carbon monoxide full combustion	$CO + \frac{1}{2}O_2 \rightarrow CO_2$
Methane electrochemical oxidation	$CH_4 + 4O^{-2} \rightarrow 2H_2O + CO_2 + 8e^-$
Carbon monoxide electrochemical oxidation	$CO + O^{-2} \rightarrow CO_2 + 2e^-$
Hydrogen electrochemical oxidation	$H_2 + O^{-2} \rightarrow H_2O + 2e^-$
Methane cracking	$CH_4 \rightarrow 2H_2 + C$
Boudouard reaction	$2CO \rightarrow CO_2 + C$

Table 4 Reaction at Cathode of an SOFC [7, 8]

Reaction	Equation
Oxygen electrochemical reduction	$\frac{1}{2}O_2 + 2e^- \rightarrow O^{2-}$

\

For a desired potential, multiple FCs are assembled together in series to form a “stack” by using interconnecting plates that helps keep the fuel at anodic side and air at the adjacent cathodic side apart in planar solid oxides fuel cells stacked together. [29]
The highest theoretical efficiency is around 80%. [1]

SO fuel cells because of their high efficiency and effectiveness in terms of cost is the most desirable for producing electrical power from a vast array of fuels. The properties, structure and morphology of cell components play a vital role to judge how the solid oxide fuel cell will perform and if it is durable or not. [30]The solid oxide fuel cell has a working temperature in the range of 800-1000 °C. To lower the cost of interconnecting plates, manifolds and seals, efforts are being made to develop SOFCs, especially smaller ones, that operate at a lower temperature range. [1]

Alongside electricity, the high operating temperature of solid oxide fuel cells produces thermal energy at higher temperatures. The thermal energy can then be utilized in different manners, for example, in cogeneration, CHP systems or in production of electrical power by driving a gas turbine. Thus, in comparison to the rest of the types of fuel cells, solid oxide fuel cells have more efficiency. Solid oxide fuel cells are also employed for the electrolysis of H_2O at high temperatures without requiring any sort of significant changes in the schematic. Various types of fuels can be utilized, solid oxide fuel cells can be brought directly into operation with hydrocarbons, and SOFCs are much more efficient than the rest of the types of FCs. These are the three most important benefits that SOFCs have over other fuel cell types. The additional advantage of SOFCs is that they have a greater tolerance to CO, which undergoes an electrochemical oxidation reaction to be converted to carbon dioxide at the positive electrode. PEMFCs on the other hand can easily be poisoned by carbon monoxide due to which results in the requirement of an advanced and costly external processing of hydrocarbons to convert carbon monoxide to carbon dioxide. Then the removal of CO_2 results in a pure H_2 to be utilized as fuel, and hence carbon dioxide emissions are reduced. Solid oxide fuel cells can greatly tolerate other impure substances that can adversely affect other FCs and can also tolerate changes in the composition of fuels due to which the requirement of external processing of fuels is generally low to almost negligible and the durability of the fuel cell is enhanced greatly. Further benefits are that the need of utilization of Pt and other expensive substances is eliminated; such substances greatly increase the cost of FCs. Since no liquids are present in the SOFCs, most of the problems related to corrosion and electrolyte loss are eliminated. Also, the methods to stack SOFCs are simpler and less expensive as compared to polymer electrolyte membrane fuel cells. [1, 31]

As mentioned above, the operating temperature range of a solid oxide fuel cell is in the range of 700-1000^{o}C.[28] When the SOFCs are operated at such elevated temperatures, thermal stresses due to mismatch of coefficient of thermal expansion (CTE) between different components and temperature gradients in the solid oxide fuel cells stack are greatly increased to higher levels. Delamination and production of cracks at a microscopic level in the various layers of solid oxide fuel cells stack are caused. Every layer of an SOFC has critical importance and a vital role to play when SOFC is being operated. Thus, to

successfully design and operate a solid oxide fuel cell, the requirement of a thorough and optimum analysis of the solid oxide fuel cell has to be fulfilled.

A lot of research has been done to analyze a solid oxide fuel cell thermally[32-36]. Such study and research-based activities [32-36] employed numerical and experimental analyzing techniques to approximate the stresses in single or multiple layers of an SOFC at room temperature and also by applying a uniform temperature gradient to a basic anode-electrode-cathode (PEN) assembly. The focus of such studies [32-36] were only those stresses caused by the mismatch of CTE between layers of electrolytes and anode/cathode at a specified temperature of operation, totally neglecting how temperature gradients have effects within the positive electrode-electrolyte-negative cathode assembly, and how heat interacts between said assemblies and interconnecting plates or other components of SOFCs . Many of the studies [37-39] employ FEM (finite element method) for the calculation of thermal stresses and thermochemical models to find the desired temperature gradients for both tubular [31] and planar [37, 38] solid oxide fuel cells. Thus, the factor of uneven temperature distribution in generation of thermal stresses within the solid oxide fuel cells can be incorporated in simulations.

The models of a single cell for the planar solid oxide fuel cells [37, 38] incorporated parts of SOFCs like interconnecting plates and positive electrode-electrolyte-cathode assemblies in a way that the effects of CTE mismatch and mechanical constraint between these parts were also included while analyzing the thermal stresses. Thus, simulations like those discussed in Refs. [37, 38]can prove to be very beneficial tools to calculate the distribution of thermal stresses thereby producing very effective results that may help greatly in the designing of a planar solid oxide fuel cells stack. But, in such studies [37, 38] to simplify the calculations, only one stack of SOFC was taken into consideration and other components such as gas seals were neglected. The planar stack of SOFC needs high temperature gas seals to join all the parts of the cell while keeping the air and the fuel separate. Thus, it can be seen that such high temperature gas seals and their effects must also be taken into account during analysis to obtain even more accurate results. A broken gas seal can cause leakage and degradation of the level of performance of a solid oxide fuel cell stack. But, this perspective has not been greatly studied from a literature point of view. Thus it is required that the importance of gas seals in the efficiency and operation of solid

oxide fuel cell be studied. It is required that while simulating, the model be as close as it can be to the practical one for accurate calculation and results of thermal stresses in planar solid oxide fuel cells stack.Just like it was discussed above, the models used in these studies [32-38] are simple and not close to the real one. In this study, we use a simpler approach like the ones used in [32-36] assuming uniform temperature profiles but using an FEA model to calculate the thermal stresses. [32-39]

CHAPTER 03 – METHODOLOGY

3.1 THERMODYNAMICS OF A FUEL CELL

Study of energetics is called thermodynamics. It is the science of the conversion of energy from one form to the other. Fuel cells, like heat engines, are energy transformation devices. Therefore, fuel cell provides basis for understanding the transformation of chemical energy intro the electrical energy. It can also be used to predict whether a reaction is spontaneous energetically or not. Moreover, thermodynamics helps in placing an upper limit for the maximum electrical energy a chemical reaction can produce. [40]

SOFCs have the potential to run on different hydrocarbons as fuels as well as H_2. Furthermore, they are also able to utilize as fuels compounds like Carbon Monoxide and Carbon Dioxide which gives them a huge advantage over other kinds of FCs that operate at low temperatures. Besides hydrocarbons, SOFC can also use liquid fuels like methanol, ethanol, liquefied petroleum gas, dimethyl ether and other common liquid fuels [41]. We are going to concentrate on pure hydrogen, methane and carbon monoxide as possible inlet fuels. The electrochemical reactions for these fuels are [42]:

Hydrogen (H_2):

At anode, the following reaction takes place

$$O^{2-} + H_2 \longrightarrow H_2O + 2e^- \quad (1)$$

The reaction at cathode is:

$$0.5O_2 + 2e^- \longrightarrow O^{2-} \quad (2)$$

The overall reaction of the cell is:

$$H_2 + 0.5O_2 \longrightarrow H_2O \quad (3)$$

Carbon Monoxide (CO):

The following reaction takes place at the anode:

$$CO + O^{2-} \longrightarrow CO_2 + 2e^- \quad (4)$$

At cathode:

$$0.5O_2 + 2e^- \longrightarrow \quad O^{2-} \quad (5)$$

The overall cell reaction is:

$$CO + \ 0.5O_2 \longrightarrow CO_2 \quad (6)$$

Methane (CH_4):

At anode:

$$CH_4 + 4O^{2-} \longrightarrow CO_2 + 2H_2O + 8e^- \quad (7)$$

At cathode:

$$\frac{1}{2}O_2 + 2e^- \longrightarrow O^{2-} \quad (8)$$

The overall cell reaction is:

$$CH_4 + 2O_2 \longrightarrow CO_2 + 2H_2O \quad (9)$$

Equations (3), (6) and (9) are of course the *combustion reactions* of hydrogen, carbon monoxide and methane, respectively, but this 'combustion' in fuel cell does not occur in the sense of burning [43].

Negatively charged electrons (e^-) are set free at the anode, as shown in the equations (1), (4) and (7), and help in producing current in the external circuit, and are consumed by the reaction taking place cathode, as shown in equation (2), (5) and (8).

Multiple cells are piled up together and are connected in a series to make compact units with required terminal EMF.

The first law can be written in the following form because fuel cell operates steadily. [40]

$$\Delta H = Q + W_{elect} \tag{10}$$

Here, P.E and K.E. terms are excluded as they are negligible, ΔH is the change in enthalpy, Q is the heat added to system and work of shaft has been replaced by the electrical work W_{elect}. If the fuel cell is operating isothermally and reversibly, [40]

$$Q = T\Delta S \tag{11}$$

Therefore, equation (10) can be rearranged as

$$W_{elect} = \Delta H - T\Delta S = \Delta G \tag{12}$$

where, ΔG is the Gibbs free energy. The transfer of heat Q to the surroundings that is needed for isothermal working of a fuel cell is:

$$Q = \Delta H - \Delta G \tag{12}$$

3.1.1 HEAT POTENTIAL OF A FUEL (ENTHALPY OF A REACTION)

"The maximum heat energy that can be extracted from a fuel is given by the fuel's enthalpy of reaction (for a constant-pressure process)." [40]

Because of the chemical reaction a large amount of chemical bonds are reconfigured. This results in change in the internal energy of the species. The heat that is given out of the system during a reaction is because of the change in its internal energy after subtracting the energy that is utilized in doing some work.

Consider the reaction of burning carbon in air. A large amount of heat is given out as a result of this combustion process. This is because the bonds reconfigure themselves. Product carbon dioxide is at a lower state of internal energy than the reactants i.e. Oxygen and Carbon. If some of this change in internal energy is used in doing some work, the rest

is given out in the form of heat of the reaction. This can be described in with a situation where a ball is rolling downwards from the top of the hill. At the top, the ball has a higher P.E but a lower K.E. As it rolls down, its P.E is converted to K.E and therefore, the ball moves from a higher state of P.E to a lower state of P.E. Heat of combustion of a reaction is the change in the enthalpy of a combustion reaction. Sometimes the change in enthalpy of a reaction is also referred to as "enthalpy of the reaction" or "heat of the reaction" [40]

The energy balance for the reaction can be written as [44]

$$\Delta H = H_{prod} - H_{react} \tag{13}$$

$$H_{prod} = \sum N_p \left(\bar{h}_f^o + \bar{h} - \bar{h}^o\right)_p \tag{14}$$

$$H_{react} = \sum N_r \left(\bar{h}_f^o + \bar{h} - \bar{h}^o\right)_r \tag{15}$$

Equation (13) expresses that the change in enthalpy is the difference between the energies of the products and the reactants. N_p and N_r are the number of moles of product p and the reactant r, respectively (when 1 mole of the fuel is utilized). They can be easily picked up from the stoichiometric reaction. $\bar{h}_f^o$ shows how much enthalpy is required to form one mole of chemical species at the reference state from the reference species and is called the "enthalpy of formation", $\bar{h}^o$ is the sensible enthalpy at the reference state and $\bar{h}$ is the sensible enthalpy at the specified state. The reference state is $25℃$ and $1\ atm$.

Consider a general reaction taking place at STP,

$$aA + bB \longrightarrow mM + nN \tag{16}$$

Change in enthalpy for this reaction can be written using equation (13), (14) and (15) can be written as

$$\Delta H° = \left[m\bar{h}_f^o(M) + n\bar{h}_f^o(N)\right] - \left[a\bar{h}_f^o(A) + b\bar{h}_f^o(B)\right] \tag{17}$$

For the calculation of $\Delta H°$, $(\bar{h} - \bar{h}^o)$ becomes zero.

$\Delta H°$ can now be calculated for electrochemical reactions of Hydrogen, Carbon Monoxide and Methane given by reactions (3), (6) and (9), respectively.

For Hydrogen,

Table 5: Calculation of Enthalpy of Combustion of Hydrogen

Substance	No. of moles N	$\overline{h_f^o}$ $kJ/kmol$ [45]	$N(\overline{h_f^o})$ $kJ/kmol$
H_2	1	0	0
O_2	0.5	0	0
			$H_{react} = \sum N_r(\bar{h}_f^o)_r = 0$
$H_2O_{(g)}$	1	–241,834	–241,834
			$H_{prod} = \sum N_p(\bar{h}_f^o)_p = -241{,}834$

Using equation (17),

$$\boxed{\Delta H° = -241{,}824\ kJ/kmol}$$

For Carbon Monoxide,

Table 6: Calculation of Enthalpy of Combustion of Carbon Monoxide

Substance	No. of moles N	$\overline{h_f^o}$ $kJ/kmol$ [45]	$N(\overline{h_f^o})$ $kJ/kmol$
CO	1	–110527	–110527
O_2	0.5	0	0
			$H_{react} = \sum N_r(\bar{h}_f^o)_r = -110527$
CO_2	1	–393522	–393522
			$H_{prod} = \sum N_p(\bar{h}_f^o)_p = -393522$

Using equation (17),

$$\Delta H = (-393522) - (-110527)$$

$$\boxed{\Delta H° = -282{,}995\ kJ/kmol}$$

For Methane,

Table 7: Calculation of Enthalpy of Combustion of Methane

Substance	No. of moles N	$\overline{h_f^o}$ $kJ/kmol$ [45]	$N(\overline{h_f^o})$ $kJ/kmol$
CH_4	1	–74873	–74873
O_2	2	0	0
$H_{react} = \sum N_r(\bar{h}_f^o)_r = -74873$			
CO_2	1	–393522	–393522
$H_2O_{(g)}$	2	–241,834	–483668
$H_{prod} = \sum N_p(\bar{h}_f^o)_p = -877190$			

Using equation (17),

$$\Delta H = (-877190) - (-74873)$$

$$\boxed{\Delta H° = -802{,}317\ kJ/kmol}$$

3.1.2 EFFECT OF TEMPERATURE ON ENTHALPY

Amount of heat any specie can absorb depends on its temperature. Therefore, it can be concluded that the heat of formation of a specie is also a function of the temperature. The change of enthalpy of a substance can be described by the heat-capacity of a substance. [42]

$$\Delta H_{f(T)} = \Delta H_f° + \int_{298.15}^{T} c_p(T)\, dT \qquad (18)$$

where, $\Delta H_{f(T)}$ is the heat of formation of a substance at any temperature T, $\Delta H_f°$ is the reference formation enthalpy of the substance at $T_o = 298.15\ K$ and c_p represents the heat capacity of the substance at constant pressure which itself is depends on the temperature.

The temperature dependence of c_p is described in Ref [44] as

$$\overline{C_p} = A + B(T) + C(T^2) + D(T^3) \qquad [kJ/kmol.K] \qquad (19)$$

Where A,B, C and D are constants and their values can be obtained for different gases from Ref [44]. T is in $Kelvins$ from 273 to T_{max}.

Table 8: Values of A, B, C and D for different gases to be used in equation (19)

Chemical Species	$T_{max}\ (K)$	A	$B\ (10^2)$	$C(10^5)$	$D\ (10^9)$
Hydrogen	1800	29.11	−0.1916	0.4003	−0.8704
Oxygen	1800	25.48	1.520	−0.7155	1.312
Carbon Monoxide	1800	28.16	0.1675	0.5372	−2.222
Carbon Dioxide	1800	22.26	5.981	−3.501	7.469
Methane	1500	19.89	5.024	1.269	−11.01
Water	1800	32.24	0.1923	1.055	−3.595

Using equation (19) and Table 8, we obtain the following graph.

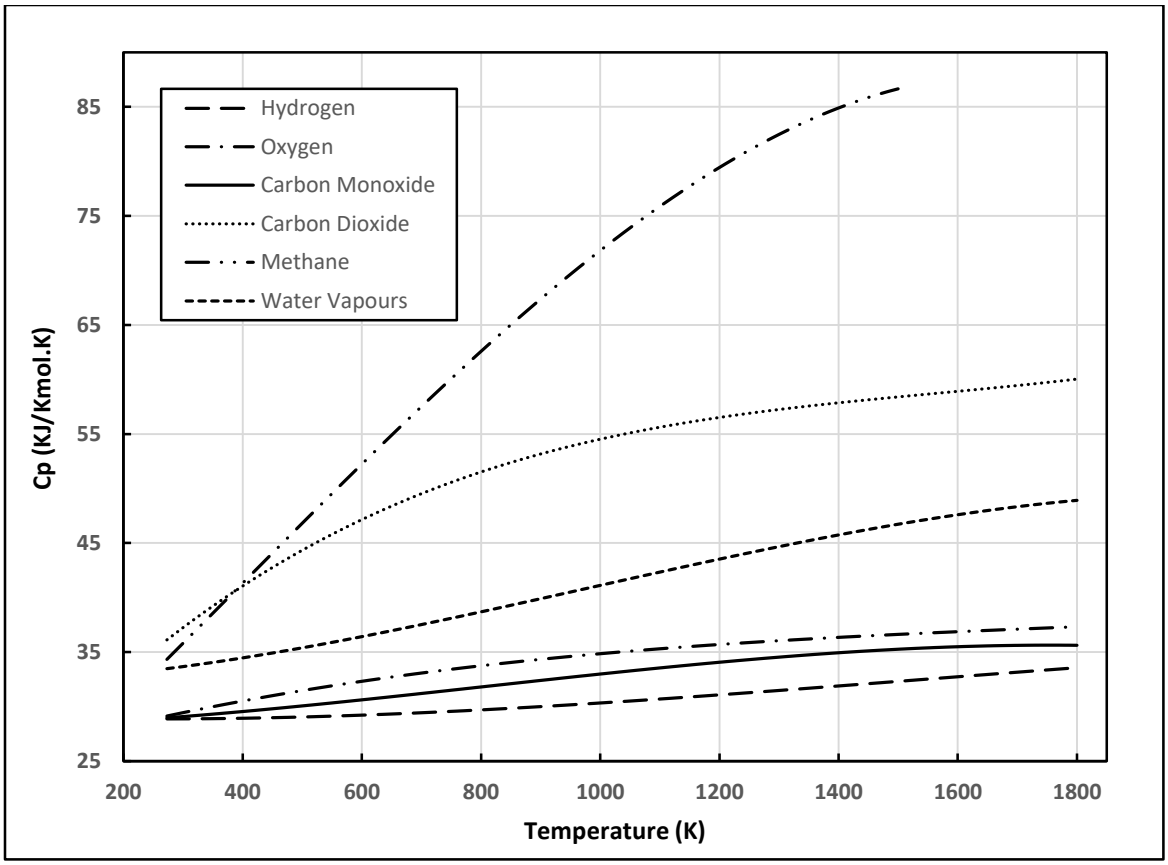

Figure 8: Specific heat (kJ/kmol.K) for different gases plotted against a temperature (K) range where equation (19) is applicable.

3.1.3 HEATING POTENTIAL

Heating potential is directly related to the enthalpy of the reaction or its heating value. It can be calculated by the following formula. [46]

$$E_{\Delta H} = \frac{-\Delta H}{nF} \tag{20}$$

$E_{\Delta H}$ represents the heating potential, ΔH is the change in enthalpy of the reaction (total heat energy), F is known as the Faradays constant (96485.334 As/mol) and n shows the number of electrons taking part in the electro-chemical reaction.

Equation (10) is used to calculate the heating voltage $E_{\Delta H}$ at 25℃ and 1 atm.

Table 9: Heating Voltage (V) calculation for three different fuels i.e. Hydrogen, Carbon Monoxide and Methane

Fuel	Overall Cell Reaction	$\Delta H°$ $kJ/kmol$	n	$E_{\Delta H}°$ (V)
Hydrogen	$H_2 + \frac{1}{2}O_2 \longrightarrow H_2O$	$-241{,}824$	2	1.2532
Carbon Monoxide	$CO + \frac{1}{2}O_2 \longrightarrow CO_2$	$-282{,}995$	2	1.4665
Methane	$CH_4 + 2O_2 \longrightarrow CO_2 + 2H_2O$	$-802{,}317$	8	1.0394

3.1.4 GIBBS FREE ENERGY

For the case of chemical reactions, only a specific amount of the energy can be transformed into the electrical energy, the rest of the energy is given out as heat. The "useful energy" that can be utilized in as electrical work is known as "Gibbs free energy". [46]

Consider equation (12),

$$\Delta G = \Delta H - T\Delta S \tag{21}$$

Here, ΔG is free available energy, ΔH is the change in enthalpy of the reaction, T is the temperature in Kelvins and ΔS represents entropy change. Equation (12) shows that the difference between ΔH and ΔG is directly related to the change of entropy. The amount of heat given out by a fuel cell operating in a totally reversible manner is the product T and ΔS. Fuel cell reactions that have negative change of entropy ΔS generate heat when the reaction takes place, while those with positive change of entropy ΔS may extract heat from the surroundings, if the irreversible heat generation is smaller than the reversible heat absorption.[42]

The Gibbs free energy can also be used in predicting the spontaneity of a chemical reaction along with the maximum electrical energy that can be obtained from the electrochemical reaction. If $\Delta G = 0$, the system is unable to produce any useful work that can be transformed into electrical energy. If ΔG is positive, some work must be done on the system for the

reaction to take place. Hence, the sign of ΔG can be used to indicate if a chemical reaction is spontaneous:

If $\Delta G\ is\ postive$, the reaction is non-spontaneous i.e not favourable energetically

If $\Delta G\ is\ zero$, the reaction takes place at an equilibrium

If $\Delta G\ is\ negative$, the reaction is spontaneous i.e favourable energetically

All reaction that are spontaneous are energetically favourable which means they are "downhill processes". Even if a reaction is spontaneous, it doesn't mean that the reaction can occur or how fast can it occur. A lot of spontaneous reactions don't take place because of the obstruction provided by some kinetic barriers. Consider the example of diamond. The reaction of transformation of diamond in to graphite is a spontaneous reaction and is energetically favourable but it doesn't occur naturally. In a similar manner, fuel-cells are also limited by kinetics of the reactions taking place. The rate of production of electricity is also limited by a number of kinetic phenomena. [40].

Under standard state conditions, we may write equation (14) as

$$\Delta G° = \Delta H° - T\Delta S° \tag{22}$$

The balance of entropy for a system that undergoes a process can be written as [44]

$$S_{gen} + (S_{in} - S_{out}) = \Delta S_{sys} \tag{23}$$

In equation (17), $S_{in} - S_{out}$ represents the net entropy transfer by heat and mass, S_{gen} is the entropy generation and ΔS_{sys} is the overall change in entropy of the system. For a reversible process, entropy generation S_{gen} is zero.

Consider this general reaction taking place at STP as shown previously in equation (16),

$$aA + bB \longrightarrow mM + nN \tag{16}$$

$$\Delta S° = [m\bar{S}°(M) + n\bar{S}°(N)] - [a\bar{S}°(A) + b\bar{S}°(B)] \tag{24}$$

The temperature dependence of ΔS can be represented as:

$$\Delta S_{(T)} = \Delta S° + \int_{298.15}^{T} \frac{c_p(T)}{T} dT \quad (25)$$

Where, $\Delta S_{(T)}$ is the change of entropy at the temperature T, $\Delta S°$ is the change in entropy at the STP, c_p is the specific heat at constant pressure as function of temperature (Equation (19)).

3.1.5 IDEAL VOLTAGE

The ideal voltage of the fuel cell shows the maximum energy that can be transformed in electrical work. It is related to the Gibbs free energy by the following equation. [47, 48]

$$E° = \frac{-\Delta G}{nF} \quad (26)$$

Where, n = number of electrons exchanged

F = Faraday's Number = 96485.33 $As\ mol^{-1}$

E^o = Ideal Voltage of the cell

3.1.6 EFFECT OF TEMPERATURE ON IDEAL VOLTAGE

Ideal voltage depends on the Gibbs free energy [Equation (26)] and Gibbs energy depends on the change in enthalpy and entropy at a temperature T at which the Gibbs free energy is calculated. Both the change in enthalpy ΔH and the change in entropy ΔS are a function of temperature as shown in equation (18) and equation (25), respectively. Therefore, ideal voltage is also a function of temperature. $\Delta H°$ and $\Delta S°$ values for the required substances are tabulated [44]

Table 10: Enthalpy and Entropy Values at STP for different gases as given in Ref [5]

Chemical Species	$\Delta H°$ $kJ/kmol$	$\Delta S°$ $kJ/kmol.K$
Hydrogen	0.0	130.571
Oxygen	0.0	205.038
Carbon Monoxide	−110527	197.544
Carbon Dioxide	−393522	213.795
Methane	−74873	186.142
Water	−241,834	188.725

3.1.7 EFFECT OF PRESSURE ON IDEAL VOLTAGE

The theoretical cell potential is not only dependent on temperature but also on the pressure. This dependency is greatly in general described by the Nernst Equation. [49]

For a reaction,

$$aA + bB \longrightarrow cC + dD \tag{27}$$

Nernst Equation can be written as

$$E = E° + \frac{RT}{nF}\ln\left[\frac{(p_A)^a(p_B)^b}{(p_C)^c(p_D)^d}\right] \tag{28}$$

For this reaction of Carbon Monoxide (6),

$$CO + \frac{1}{2}O_2 \longrightarrow CO_2 \tag{6}$$

Nernst Equation can be written as

$$E = E° + \frac{RT}{2F}\ln\left[\frac{(p_{CO})(p_{O_2})^{\frac{1}{2}}}{(p_{CO_2})}\right] \tag{29}$$

Introducing a system pressure p_{sys} and defining $p_{CO} = \alpha p_{sys}$, $p_{O_2} = \beta p_{sys}$ and $p_{CO_2} = \gamma p_{sys}$, equation (23) can be rearranged as

$$E = E° + \frac{RT}{2F}\ln\left[\frac{\alpha.\beta^{\frac{1}{2}}}{\gamma}\right] + \frac{RT}{4F}\ln\left[p_{sys}\right] \quad (30)$$

If $\alpha, \beta \; and \; \gamma$ are constants, increasing system pressure from p_1 to p_2 influences the cell potential as follows

$$\Delta E = \frac{RT}{4F}\ln\left[\frac{p_2}{p_1}\right] \quad (31)$$

3.1.8 IDEAL EFFICIENCY OF A FUEL CELL

The reversible electrical efficiency of a fuel cell at a pressure *p* and temperature *T*, can be given by the following equation [50]

$$\eta = \frac{Total\ energy\ that\ can\ be\ used}{Total\ energy\ that\ is\ available} \quad (32)$$

We know that the total useful energy is the Gibbs free energy and total available energy is the change in enthalpy of the reaction, so now we can equation (32) as:

$$\eta = \frac{\Delta G}{\Delta H} \quad (32)$$

Ref [51] calls this efficiency as “the maximum efficiency possible” or “maximum efficiency limit”

3.2 THERMAL ANALYSIS OF A SOLID OXIDE FUEL CELL

A typical unit cell of a planar SOFC stack is composed of a positive electrode, an electrolyte, a negative electrode (known as PEN assembly), interconnect plates and seals. In practical applications, multiple cells are assembled in the form of a stack. An SOFC operated between the temperature range of 700-1000 C [52]. The high temperature operation gives rise to a significant level of thermal stresses due to mismatch of coefficient of thermal expansion (CTE) between different components and temperature gradients in the SOFC system. These kind of thermal stresses can cause delamination and micro-cracking in different layers of the PEN assembly, each of which is very critical to the operation of an SOFC. Hence, a comprehensive thermal analysis of an SOFC stack is required for the successful design and operation of an SOFC.

A number of studies have been carried out on the thermal analysis of an SOFC [53-60]. Most of these studies [53-57] used experimental and numerical analysis to calculate or estimate the stresses in the electrolyte or electrolyte layers at either room temperature or by applying a uniform temperature gradient within a simple positive electrode-electrolyte-negative electrode assembly. These studies [53-57] only focused on the stresses caused by the mismatch of coefficient of thermal expansion between electrolyte and electrode layers for a given operating temperature ignoring the effects of temperature gradients within the PEN assembly and thermal interactions between PEN and the other components of the cell, like interconnects. A number of studies [58-60] use Finite Element Analysis to calculate the thermal stresses and thermo-chemical models to establish the required temperature profiles for planar [58, 59] and tubular [60] SOFCs. As a result, the contribution of uneven temperature distribution in the generation of thermal stresses within the SOFC can be included and simulated.

These models of a single cell for the planar SOFCs [58, 59]included components like interconnects and PEN such that the effects of coefficient of thermal expansion mismatch and mechanical constraint between these the components were also taken into account in the thermal stress analysis. Hence, simulation approaches like the ones proposed in Refs. [58, 59]would provide a very effective tool for calculation of thermal stress distribution and give very useful results for design of planar SOFCs. However, in these studies [58,

59], for the sake of simplicity of calculation, only a single stack of cell was considered and the other parts as gas seals were not included. The planar type of SOFC require high temperature gas seals to bond the cell components and separate the air and fuel compartments. Therefore the influence of these gas seals on the thermal stress distribution also need to be evaluated to obtain highly accurate results. If a gas seal is damaged, it may cause leaked and degrade the performance of an SOFC. However this issue lacks sufficient studies in the literature and hence provides a need for study of the role of gas seals in the efficient working and durability of an SOFC. To provide an effective tool for the calculation of thermal stress in a planar SOFC cell, it would be better to use a simulation model as close as possible to the practical one. As described above, the models used in prior in these studies [53-60] have been simplified to some extent. In this study, we use a simpler approach like the ones used in [53-57] assuming uniform temperature profiles but using an FEA model to approximate the thermal stresses. [58-60]

3.2.1 THEORETICAL ANALYSIS

Our primary aim is to analyze the shear stress that develops between the layers of a fuel cell. A model of our situation is illustrated in the following figures:

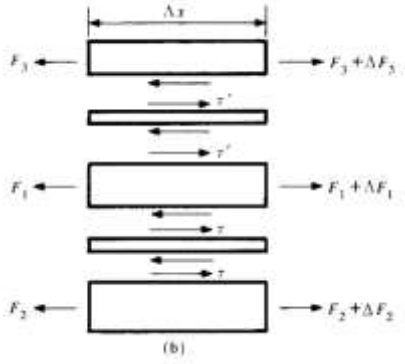

Figure 9: Free-body Diagram of Fuel Cell

We begin with a simple force balance on the individual components of the fuel cell including the electrolyte, the anode and the cathode [61].

$$\frac{dF_1}{dx} + \tau' - \tau = 0$$

$$\frac{dF_2}{dx} + \tau = 0$$

$$\frac{dF_3}{dx} - \tau' = 0$$

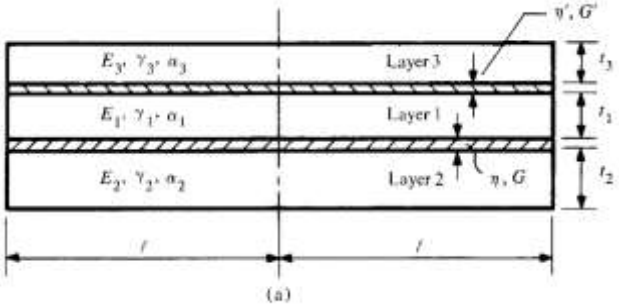

Figure 10: Schematic of Fuel Cell

Furthermore, the stress-strain relationships for each of the three layers are: [61]

$$\frac{du_1}{dx} = \frac{F_1}{E_1 t_1} + \alpha_1 T$$

$$\frac{du_2}{dx} = \frac{F_2}{E_2 t_2} + \alpha_2 T$$

$$\frac{du_3}{dx} = \frac{F_3}{E_3 t_3} + \alpha_3 T$$

The Shear Stress relationships are defined as follows:

$$\frac{\tau}{G} = \frac{u_1 - u_2}{\eta}$$

$$\frac{\tau'}{G'} = \frac{u_3 - u_1}{\eta'}$$

The solution of the above equations is as follows:

$$\tau = A_1 \sinh \beta_1 x + A_2 \sinh \beta_2 x + A_3 \cosh \beta_1 x + A_4 \cosh \beta_2 x$$

$$\tau' = A_1 k_1 \sinh \beta_1 x + A_2 k_2 \sinh \beta_2 x + A_3 k_3 \cosh \beta_1 x + A_4 k_4 \cosh \beta_2 x$$

β_1 and β_2 are constants that can be solved by finding the roots of the following equation:[61]

$$\beta^4 - \frac{1}{E_1 t_1}\left[\frac{G}{\eta}\left(1 + \frac{E_1 t_1}{E_2 t_2}\right) + \frac{G'}{\eta'}\left(1 + \frac{E_1 t_1}{E_3 t_3}\right)\right]\beta^2 + \frac{GG'}{(E_1 t_1)^2 \eta\eta'}\left[\left(1 + \frac{E_1 t_1}{E_2 t_2}\right)\left(1 + \frac{E_1 t_1}{E_3 t_3}\right) - 1\right] = 0$$

We assume:

- *The materials are isotropic and homogeneous.*
- *The ends are free.*
- *Linear elastic behavior is exhibited by the materials*
- *The contact with the interconnect is frictionless*

This allows us to simplify our system and the constants A_3, A_4, k_3 and k_4 are equal to zero. The shear stress between the layers is thus:

$$\tau = C_1 \frac{\sinh \beta_1 x}{\cosh \beta_1 l} + C_2 \frac{\sinh \beta_2 x}{\cosh \beta_2 l}$$

$$\tau' = C_1 k_1 \frac{\sinh \beta_1 x}{\cosh \beta_1 l} + C_2 k_2 \frac{\sinh \beta_2 x}{\cosh \beta_2 l}$$

The constants k_i, C_1, C_2 are calculated as follows:

$$k_i = E_1 t_1 \left[\left(\frac{1}{E_1 t_1} + \frac{1}{E_2 t_2}\right) - \frac{\beta_i \eta}{G}\right]$$

$$C_1 = \frac{G\beta_1[D_2 k_2 + D_3]}{E_1 t_1 \eta\left({\beta_1}^2 - {\beta_2}^2\right)}$$

$$C_2 = \frac{G\beta_2[D_2 k_1 + D_3]}{E_1 t_1 \eta\left({\beta_2}^2 - {\beta_1}^2\right)}$$

Similarly, the constants D_1, D_2 and D_3 are calculated as follows:

$$D_1 = \frac{E_1 t_1 [E_3 t_3 (\alpha_3 - \alpha_1) + E_2 t_2 (\alpha_2 - \alpha_1)] T}{E_1 t_1 + E_2 t_2 + E_3 t_3}$$

$$D_2 = \frac{E_2 t_2 [E_1 t_1 (\alpha_1 - \alpha_2) + E_3 t_3 (\alpha_3 - \alpha_2)] T}{E_1 t_1 + E_2 t_2 + E_3 t_3}$$

$$D_3 = \frac{E_3 t_3 [E_1 t_1 (\alpha_1 - \alpha_3) + E_2 t_2 (\alpha_2 - \alpha_3)] T}{E_1 t_1 + E_2 t_2 + E_3 t_3}$$

3.2.2 PARAMETERS USED

The following cell parameters were fixed:

Table 11: Parameters used for Thermal Analysis

Layer/Parameter	Thickness (mm)	Temperature (C)	Material
Interconnect	10	22 – 800 (ramped)	Structural Steel
Electrolyte	0.5	22 – 800 (ramped)	Yttria-stabilised Zirconia (YSZ)
Anode	0.1	22 – 800 (ramped)	Ni-YSZ
Cathode	0.1	22 – 800 (ramped)	Varies

The properties of the materials used are as follows:

Table 12: Properties of materials used in Thermal Analysis

Material / Properties	Layer	Density (g/cm^3)	Young Modulus (GPa)	Shear Modulus (GPa)	Thermal Expansion Coefficient 10^{-5} (K^{-1})	Thermal Conductivity (W/mK)
Structural Steel [62]	Interconnect	7.85	200	76.9	1.2	60.5
Yttria-stabilised Zirconia (YSZ) [63]	Electrolyte	6.1	130	55	1	2
Ni – YSZ composite (40% porous) [63]	Anode	8.05	50	17.5	1.25	4

Ni – YSZ composite (26% porous) [63]	Anode	8.20	90	37	1.3	6
Porous Platinum [63]	Cathode	21.45	171	61.5	0.91	69.1
Zirconium Dioxide [64]	Cathode	5.6	200	76.3	1.05	3
Strontium Doped Lanthanum Manganite [65]	Cathode	5.3	35	12.9	1.17	10

The maximum shear strength of each material is (according to convention) 60% of the tensile strength and is tabulated as follows:

Table 13: Shear strength of materials used in Thermal Analysis

Material	Shear Strength (MPa)
Yttria-stabilised Zirconia (YSZ) [63]	165
Ni – YSZ composite (40% porous) [63]	70
Ni – YSZ composite (26% porous) [63]	70
Porous Platinum [63]	100
Zirconium Dioxide [63, 64]	400
Strontium Doped Lanthanum Manganite [65]	93

3.2.3 ANSYS MODEL

- The basic geometry consisted of the fuel cell sandwiched between two interconnects that were bolted.
- The bolts were subjected to pretension and the fuel and air inlets were the fixed supports.

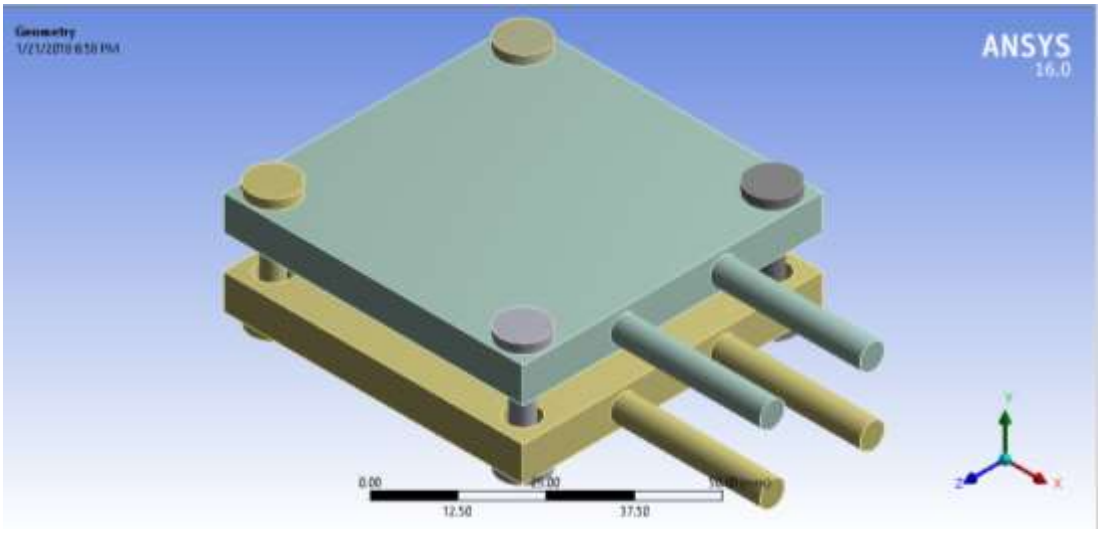

Figure 11: Geometry of the ANSYS Model of Fuel Cell

3.3 PERFORMANCE OF A SOLID OXIDE FUEL CELL

The performance of a solid oxide fuel cell is a function of many of its variables including:

- Flow rates of fuel and air/oxygen.
- Geometry of the fuel cell
- Interconnect coverage area
- Conductivity of the different layers
- Weight fraction of fuel and oxygen etc

Any attempt at optimizing the performance of a fuel cell will be incomplete without a parametric study of how these factors affect its performance and the optimum mix of all the factors.

3.3.1 GOVERNING EQUATIONS

A complete model of a fuel cell incorporates all the necessary parameters that could possibly enhance or degrade it. It is therefore a complex model that encompasses the electrochemical and mass diffusion elements and must be solved simultaneously to obtain a suitable solution.

3.3.2 ELECTROCHEMICAL MODEL [44, 66-74]

An ideal fuel cell is able to maintain its voltage irrespective of the current that is drawn from it. In reality, however, the voltage of the fuel drops due to irreversible losses and are known as overpotential losses.

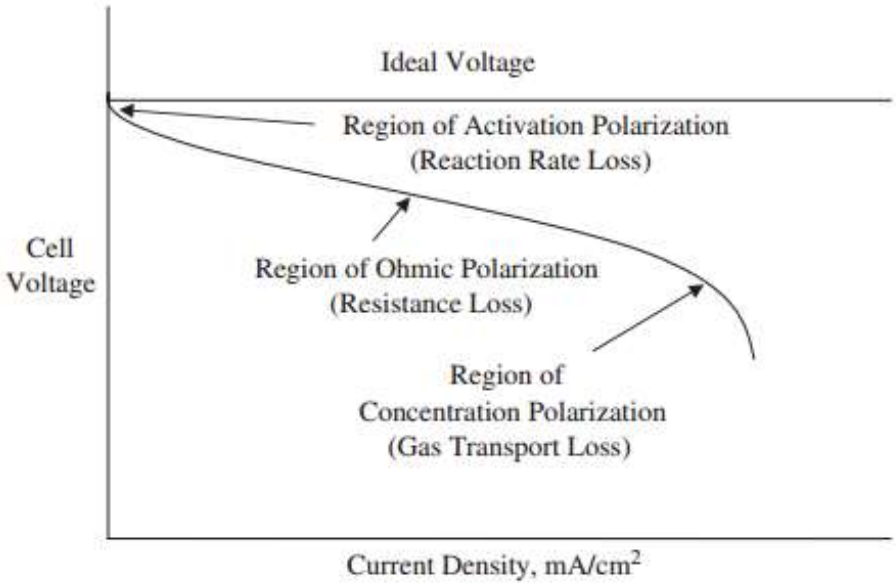

Figure 12: Cell Voltage to current density (Theoretical) [75]

The activation loss can be calculated as follows:

$$j = j_0 \left[\exp\left(\frac{\alpha n F \eta}{RT}\right) - exp\left(-\frac{(1-\alpha) n F \eta}{RT}\right)\right]$$

It can be rearranged to represent the activation potential as:

$$\eta_{act} = \left(\frac{RT}{n\alpha_a F}\right) \ln\left(\frac{j}{j_{0a}}\right) - \left(\frac{RT}{n\alpha_c F}\right) \ln\left(\frac{j}{j_{0c}}\right)$$

The Ohmic polarization is as follows:

$$\eta_{ohm} = jASR_{ohm}$$

Similarly, the concentration polarization is as follows:

$$\eta_{conc} = c \ln \frac{j_L}{j_L - j}$$

Here c is a constant equal to:

$$c = \frac{RT}{nF}\left(1 + \frac{1}{\alpha_i}\right)$$

The combined effect of these overpotentials/polarizations is to reduce the voltage of the fuel cell that we have previously calculated. The new voltage of the fuel cell is calculated as follows:

$$V = E_{Th} - \eta_{act} - \eta_{ohm} - \eta_{conc}$$

Here E_{TH}, the theoretical open circuit voltage is calculated as follows:

$$E_{Th} = V_{oc} + \frac{RT}{nF} \ln \frac{\prod a_{products}^{v_i}}{\prod a_{reactants}^{v_i}}$$

3.3.3 TRANSPORT EQUATIONS

Seven different regions are considered including:

- Upper interconnect
- Lower interconnect
- Oxygen/air flow area
- Fuel flow area
- Cathode
- Anode
- Electrolyte

The pressure gradients that are created and the high temperatures warrant a compressible flow analysis and the assumption of incompressible flow is not possible here. Steady flow is considered to simplify the model.

The mass momentum and energy equations are to be applied to each of the regions (where applicable) and the resulting system of equations is to be solved simultaneously.

Oxygen and Fuel

The following assumptions are made:

- No chemical reaction occurs within the flow channels and it is restricted to the cathode and anode.

- The consumption of oxygen and carbon monoxide will not significantly change the density of the mixture.
- The flow itself is slightly compressible.

The mass equation is therefore:

$$\frac{\partial \rho}{\partial t} + \nabla \cdot (\rho \mathrm{V}) = S_m$$

Similarly, the momentum equation is as follows:

$$\frac{\partial}{\partial t}(\rho V) + \nabla \cdot (\rho \mathrm{VV}) = -\nabla p + \rho \vec{g} \nabla \cdot \vec{\tau} + \vec{S}_M$$

The stress tensor of the system is equal to:

$$\vec{\tau} = \mu[(\nabla V + \nabla V^T) - \frac{2}{3}\nabla . V]$$

Each species must be conserved and so the species conservation equation is:

$$\frac{\partial}{\partial t}(\rho c_i) + \nabla \cdot (\rho \mathrm{V} c_i) = -\nabla \cdot \vec{J}_i + S_{s,i}$$

The energy equation is equal to:

$$\frac{\partial}{\partial t}(\rho e) - \frac{\partial p}{\partial t} + \nabla \cdot (\rho \mathrm{V} e) = \nabla \cdot (k^{eff} \nabla T) + S_e + S_{rad}$$

The above equations apply both to the anode and the cathode and must be applied to both of them separately. Boundary conditions, initial conditions and flow and fluid properties will generally be different in both channels and the equations will therefore have to be adjusted accordingly.

Electrodes

The porous nature of the electrodes allows ions to be transported across them and the reaction is considered to be completely contained within the electrodes and is assumed to not occur in the flow regions. Therefore, it is imperative that we write the basic mass, momentum, energy and species equations for the electrodes as well.

The mass equation is as follows:

$$\frac{\partial}{\partial t}(\rho\varepsilon) + \nabla \cdot (\rho\varepsilon \mathrm{V}) = 0$$

The momentum equation comes out to be:

$$\frac{\partial}{\partial t}(\rho\varepsilon \mathrm{V}) + \nabla \cdot (\rho\varepsilon \mathrm{V}\mathrm{V}) = -\varepsilon\nabla p + \nabla \cdot (\varepsilon\zeta) + \frac{\varepsilon^2 \mu \mathrm{V}}{\kappa}$$

The species balance equation is as follows:

$$\frac{\partial}{\partial x}(\rho\varepsilon c_i) + \nabla \cdot (\rho\varepsilon \mathrm{V} c_i) = -\nabla \cdot \varepsilon\vec{J}_i + S_{s,i}$$

Finally, the energy equation is as follows:

$$\frac{\partial}{\partial t}(\rho\varepsilon e) - \varepsilon\frac{\partial p}{\partial t} + \nabla \cdot (\rho\varepsilon V e) = \nabla \cdot \varepsilon\left(k_{eff}\nabla T - \sum_i h_i\vec{J}_i\right) + S_e + S_{rad}$$

Electrolyte

The electrolyte plays the important role of separating the cathode and the anode while also providing a path to the oxygen ions to go through, ideally, unhindered. Governing equations for analysis of the electrolyte can be derived from Ohm's law, conservation of charge and it is also important to consider the energy balance:

$$j_{io} = -\sigma_{io}^{eff}\nabla\emptyset_{io}$$

$$\nabla \cdot \left(\sigma_{io}^{eff}\nabla\emptyset_{io}\right) = S_{io}$$

$$\frac{d}{dx}\left(-A_e k_e \frac{dT_e}{dx}\right)\Delta x = q_{e-ele,a} + q_{e-ele,c} + q_{conv.ele,a} + q_{conv,ele,c} + q_{rad,e} + q_{gen,e} + q_{e,joule}$$

Interconnects

No ions pass through the interconnect. It is used only to allow current to pass through. Therefore, in a similar manner to that of the electrolyte, analysis of the interconnect depends primarily on the same governing equations and can be expressed as follows:

$$j_{el} = -\sigma_{el}^{eff} \nabla \emptyset_{el}$$

$$\nabla \cdot \left(\sigma_{el}^{eff} \nabla \emptyset_{el}\right) = S_{el}$$

$$\frac{d}{dx}\left(-A_{int} k_{int} \frac{dT_{int}}{dx}\right) \Delta x = q_{int-ele} + q_{conv,chan} + q_{rad,chan} + q_{gen,int} + q_{int,joule}$$

The electric current density of the interconnect is related to the ionic charge density of the electrolyte be the following equation:

$$\nabla \cdot j_{io} = -\nabla \cdot j_{el}$$

3.3.4 DIFFUSION MODELS

There are several diffusion models that can be utilized. Fick's diffusion model [2] allows for a simple analysis yielding reasonably practical results. It is defined as:

$$\vec{N}_i = -CD_{i,j} \nabla X_i$$

In the case of binary systems [3], it is redefined as:

$$\vec{N}_i = -CD_{i,mixture} \nabla X_i + X_i \sum_{j=1}^{n} N_j$$

The other model and the one utilized in our study is the Stefan-Maxwell model [4]. It is more practical for multicomponent systems and allows for a greater degree of accuracy and is defined as follows:

$$-\nabla X_i = \sum_{j=1, j \neq i}^{n} \frac{X_j N_i - X_i N_j}{CD_{i,j}}$$

3.3.5 ANALYSIS

The sophisticated equations warrant a numerical analysis and while the inherent approximations and assumptions may introduce a certain amount of error into our results. It is nevertheless a necessity and a compromise between accuracy and the need to find a practical result and the model can be used to predict the trend that exists between the different parameters and the fuel cell performance.

3.3.6 PARAMETERS

For the sake of simplicity, the following factors were fixed:

- Anode: Ni/YSZ – 26% porous
- Cathode: Strontium doped Lanthanum Manganite
- Temperature of the fuel cell: 800 C
- Permeability of cathode: 1E-10 m^2
- Permeability of anode: 1E-10 m^2
- Fuel flow rate: 1 mL/s
- Oxygen flow rate: 1 mL/s

The properties of the multiple gases involved in the fuel cell are as follows:

Table 14: Fuel Cell Gas Properties

Gas/Properties	Molecular Mass	Diffusion Volume (10^{-3} m^3/kg.atom)
Oxygen [4]	32	16.6
Nitrogen [5]	28	17.9
Carbon Dioxide [6]	44	26.9
Carbon Monoxide [7]	28	18.9
Water [8]	18	12.7

The properties of dry air [9] as a function of temperature have been included in the appendix.

The diffusion constants [10] are calculated using the following equation:

$$D_{ij} = T^{1.75}\left(\frac{\sqrt{\frac{1}{M_i}+\frac{1}{M_j}}}{\left(P\left(\sqrt[3]{v_i}+\sqrt[3]{v_j}\right)\right)^2}\right)$$

Here, v_i is the diffusion volume of coponent 'i'. This yields diffusivities of:

- $D_{O_2-N_2}$= 1.950E-4 m^2/s
- D_{CO-CO_2}= 1.518E-4 m^2/s

The matrix for diffusivities in the cathode is therefore:

$$\begin{pmatrix} 1 & D_{O_2-N_2} \\ D_{O_2-N_2} & 1 \end{pmatrix}$$

If the humidity of air is to be considered, the following matrix is obtained for the cathode:

$$\begin{pmatrix} 1 & D_{O_2-H_2O} & D_{O_2-N_2} \\ D_{O_2-H_2O} & 1 & D_{H_2O-N_2} \\ D_{O_2-N_2} & D_{H_2O-N_2} & 1 \end{pmatrix}$$

However, for our purposes, humidity is ignored and either dry air or completely pure oxygen is supplied. Similarly, for the anode, we have the diffusivity matrix as:

$$\begin{pmatrix} 1 & D_{CO_2-CO} \\ D_{CO_2-CO} & 1 \end{pmatrix}$$

3.3.7 COMSOL MODEL

A COMSOL Multiphysics model was used for the complete analysis of the fuel cell. The geometry of the fuel cell was fixed according to typical values usually found in most fuel cells. The geometry of the fuel cell was as follows:

- Length of fuel cell: 0.02 m
- Channel Width: 0.4 mm
- Rib Width: 0.4 mm
- Thickness of Electrodes: 0.1 mm
- Thickness of Electrolyte: 0.1 mm

So a 50% rib area coverage ratio was assumed. The geometry is as follows:

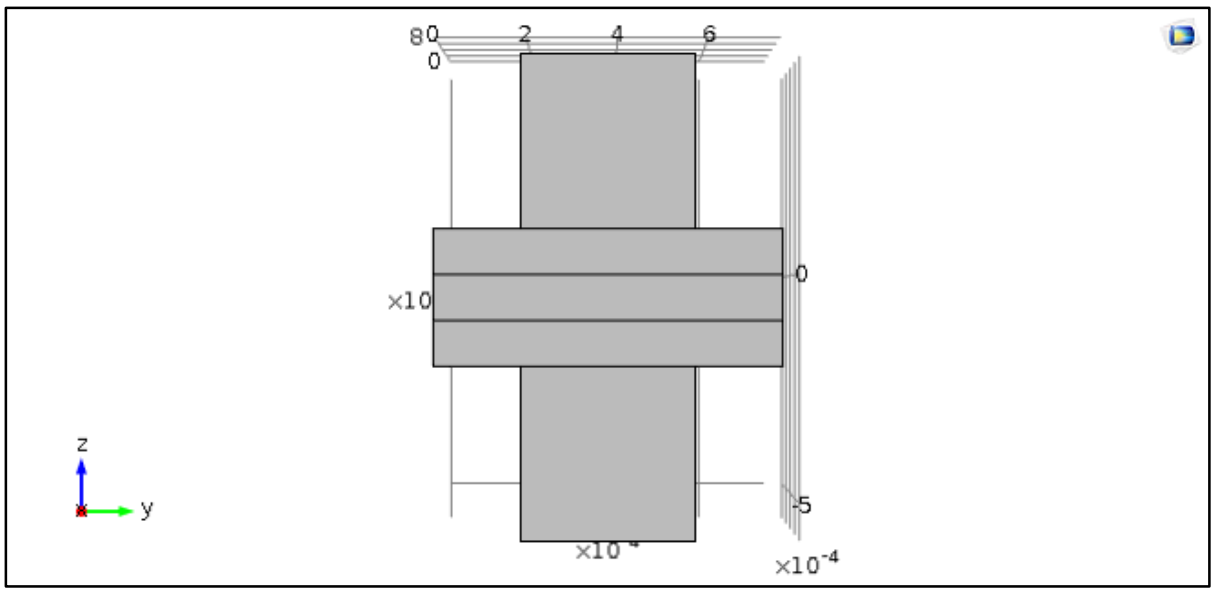

Figure 13: Fuel Cell Performance Model Dimensions

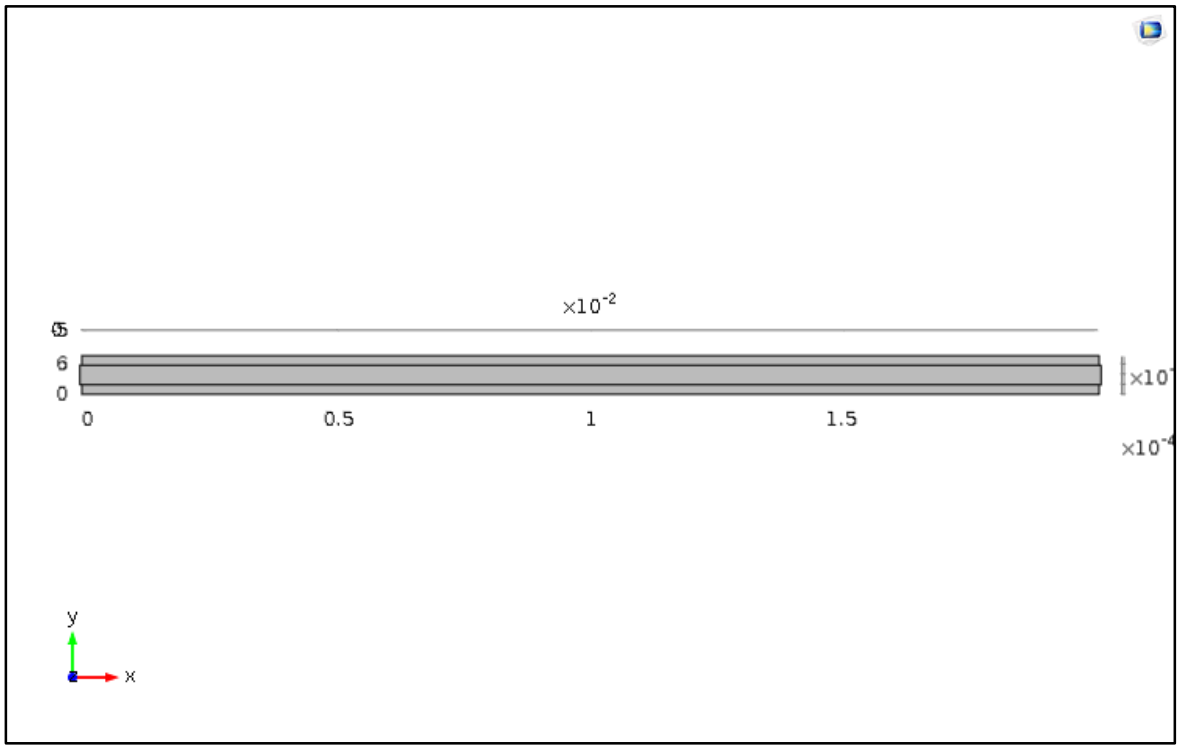

Figure 14 Fuel Cell Performance Model Length

The gasifier was not modelled in comsol and instead the weight fractions of carbon dioxide and carbon monoxide produced by the reverse boudouard reaction in the gasifier were determined. The equation of the reaction is as follows:

$$CO_2 + C \rightarrow 2CO$$

The reaction constant [11] for the forward reaction is as follows:

$$log_{10}(K_{fwd}) = \frac{9141}{T} + 0.000224T - 9.595$$

The reaction constant of the reverse reaction, therefore, will be:

$$K_{rvs} = \frac{1}{K_{fwd}}$$

The weight fraction of carbon monoxide will the be calculated as:

$$Weight\ Fraciton = \frac{K_{rvs} * 28}{K_{rvs} * 28 + 44}$$

The appendix contains the reaction constant for the reverse reaction tabulated against the temperature. Our model was used to predict the performance of the fuel cell when the gasifier was operated at a temperature of 600 C, 800 C and 1000 C with dry air at the cathode. It was also analysed at a gasifier temperature of 1000 C with pure oxygen at the cathode.

CHAPTER 04 – FABRICATION AND PROCUREMENT

The system required the fabrication or procurement of several different components. The main components have been listed below:

4.1 MUFFLE FURNACE FOR A FUEL CELL

Muffle Furnaces with a gate that allows gas inlet and outlet allowed us an easy and relatively cheap option for providing the required temperature for our fuel cell. The small chamber size meant that heating could be achieved quickly and efficiently. The gate was left slightly open so that any leakage of gas would escape quickly rather than building up and causing an accident.

Figure 15: Fuel Cell Furnace

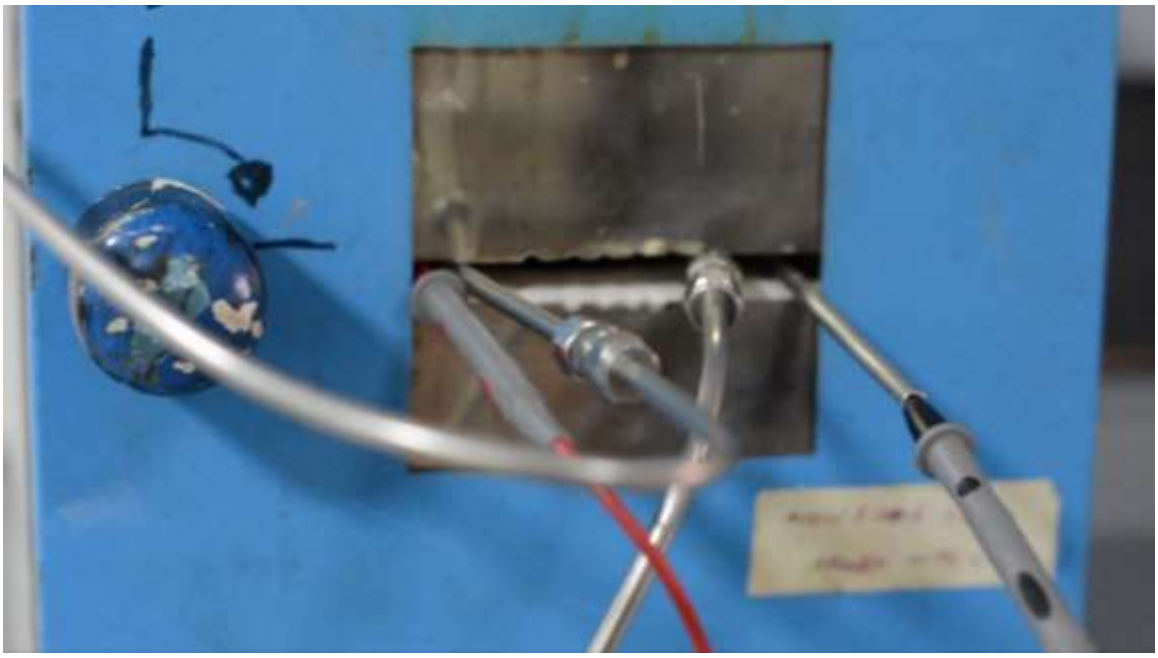

Figure 16: Muffle Furnace Gate

4.2 TUBE FURNACE FOR A GASIFIER

A tube furnace on the other hand provided the best option for our gasifier. The muffle furnaces available had very small chamber sizes not suitable for our gasifier. Alternatively, tube furnaces allowed us to use the entire tube as our gasifier. This greatly increased the reaction site of our gasifier and allowed efficient conversion of carbon dioxide to carbon monoxide via carbon capturing.

Figure 17: Tube Furnace and Muffle Furnace

Figure 18: Gasifier

4.3 MASS FLOW CONTROLLER

A Mass Flow Controller accurately controls the mass flow rate and accounts for changes in pressure and temperature accurately. These are however relatively expensive. We instead opted for a rotameter that can fairly accurately control the volume flow rate. As the total mass flowing through is a function of both the temperature and the pressure of the fluid, the mass flow rate may change as the volume flow rate stays constant. However, as our pressure and temperature were constant throughout testing, the rotameter proved to be a very cheap and accurate alternative for mass flow controllers in our scenario.

Figure 19: Mass Flow Controller

4.4 INCONEL 625 WIRE MESH

The Inconel 625 is a nickel-chromium-molybdenum-niobium alloy with excellent resistance to inorganic acid, pitting, crevice corrosion and good processing performance. It allowed us to prevent solid particles from entering the gasifier and another filter at the exit of the gasifier allowed us to protect the fuel cell from impurities and extend its lifespan.

Figure 20: Inconel 625 Wire M**esh**

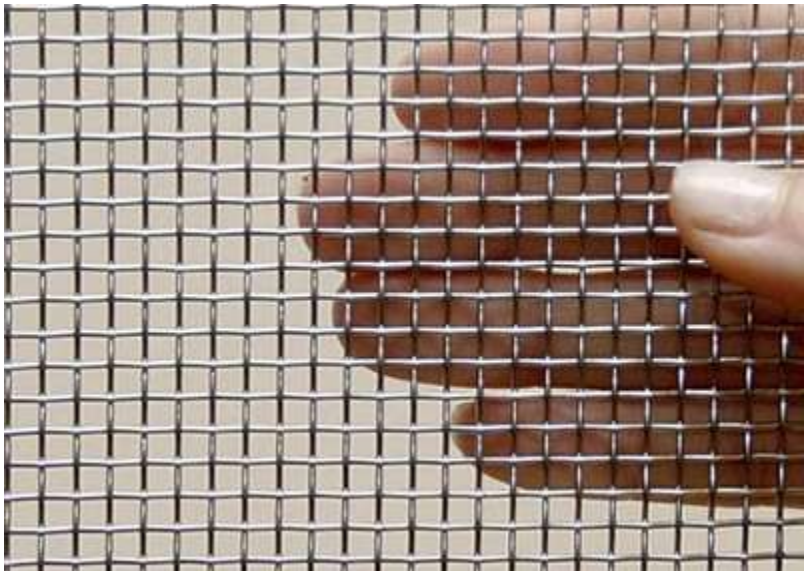

Figure 21: Wire Mesh Closeup

4.5 FUEL CELL FABRICATION

The Fuel Cell was fabricated using LNCZ (Lithium Nickel Copper Zinc) composite for both the anode and the cathode. The fuel cell was then sintered and nickel foam was then coated on the anode. The cathode, anode and the electrolyte were first separately deposited. Each layer was made 2 mm thick and the diameter of the fuel cell was 13 mm. A larger fuel cell would have yielded greater power but also significantly increased the complexity of manufacturing. Button fuel cells provide reasonable mechanical strength and despite their low power, their current and power density can still be used as metrics to measure the performance.

4.6 FUEL CELL HOLDER

The Fuel Cell holder was designed to allow easy inlet and escape of the reactant and product gases. It was also imperative that the fuel cell was securely clamped. The fuel cell was clamped between two dies that each had an inlet tube and an exit tube welded to them. The dies also functioned as a current collector and allowed us to perform our conductivity and power tests with negligible resistance and therefore negligible power loss.

Figure 22: Fuel Cell Holder

CHAPTER 05 – TESTING

5.1 CONDUCTIVITY TESTING

Applying the conventional four-point-probe method to measure the in-plane conductivity of various membranes and/or conductivity performance in various environment. We were successfully able to measure voltage drop and the resistance of the fuel cell in order to optimize the running of the fuel cell. The muffle furnace was used in the conductivity test.

Figure 23: Four Probe Conductivity Test

5.2 LOAD CELL TESTING

Load Cell Testing of the Fuel provided a parametric with which to compare our fuel cell performance to a typical fuel cell performance. It provided us with a measurement of the

power density and the voltage correlated with the current density or the current that we needed to extract from the fuel cell.

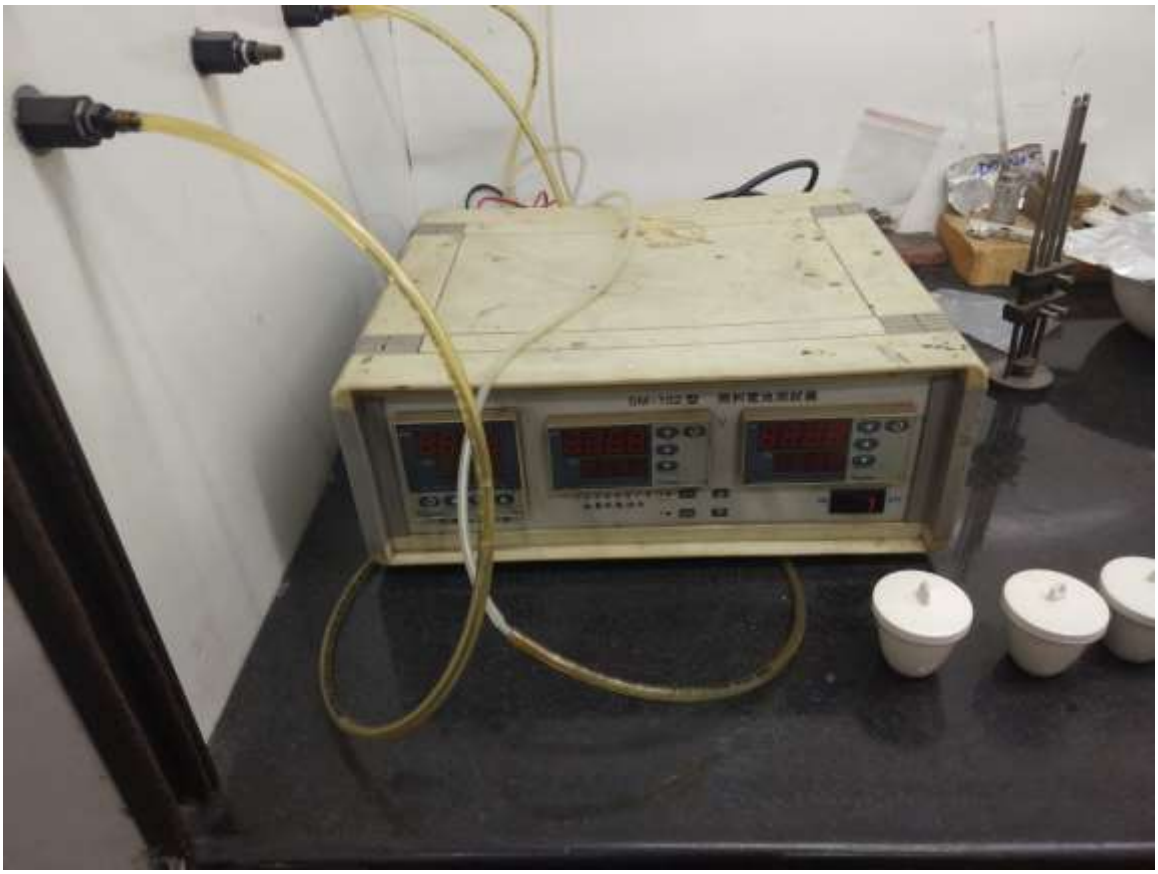

Figure 24: Load Cell Testing Equipment

CHAPTER 06– RESULTS AND DISCUSSIONS

6.1 THERMODYNAMICS OF A FUEL CELL

6.1.1 IDEAL VOLTAGE

Using equation (26) and (22), $\Delta H°$ (as previously calculated), using equation (24) and thermodynamic tables given in Ref [44], $E°$ is calculated for three different fuels.

Table 15: Ideal Voltage (V) for three different fuels i.e. Hydrogen, Carbon Monoxide and Methane

Fuel	Overall Cell Reaction	$\Delta H°$ $kJ/kmol$	$\Delta S°$ $kJ/kmol.K$	n	$\Delta G°$ $kJ/kmol$	$E°$ (V)
Hydrogen	$H_2 + \frac{1}{2}O_2 \longrightarrow H_2O$	$-241{,}824$	-44.365	2	-228606.6	1.1847
Carbon Monoxide	$CO + \frac{1}{2}O_2 \longrightarrow CO_2$	$-282{,}995$	-86.267	2	-257274.4	1.3332
Methane	$CH_4 + 2O_2 \longrightarrow CO_2 + 2H_2O$	$-802{,}317$	-4.973	8	-800834.4	1.0375

The ideal voltage of different fuels is different. As seen in the methodology section, the ideal voltage depends on the Gibbs free energy of a reaction. Methane has the highest amount of Gibbs free energy available. But its reaction involves eight electrons which decreases the voltage.

The maximum voltage is obtained when Carbon Monoxide is used as a fuel.

6.1.2 TEMPERATURE DEPENDENCE OF IDEAL VOLTAGE

ΔH and ΔG values can be obtained at different temperatures by making use of equations (17), (18), (19), (21), (24), (25) and (26).

$$\Delta H° = \left[m\bar{h}_f^o(M) + n\bar{h}_f^o(N)\right] - \left[a\bar{h}_f^o(A) + b\bar{h}_f^o(B)\right] \quad (17)$$

$$\Delta H_{f(T)} = \Delta H_f° + \int_{298.15}^{T} c_p(T)\, dT \quad (18)$$

$$\overline{C_p} = A + B(T) + C(T^2) + D(T^3) \tag{19}$$

$$\Delta G = \Delta H - T\Delta S \tag{21}$$

$$\Delta S° = [m\bar{S}°(M) + n\bar{S}°(N)] - [a\bar{S}°(A) + b\bar{S}°(B)] \tag{24}$$

$$\Delta S_{(T)} = \Delta S° + \int_{298.15}^{T} \frac{c_p(T)}{T} dT \tag{25}$$

$$E° = \frac{-\Delta G}{nF} \tag{26}$$

Values of ΔH, ΔG, $E_{\Delta H}$ and E for three different fuels (Hydrogen, Carbon Monoxide and Methane) are calculated and tabulated in APPENDIX I. The following figure shows a plot of Fuel Cell Voltage against the Temperature of the fuel Cell.

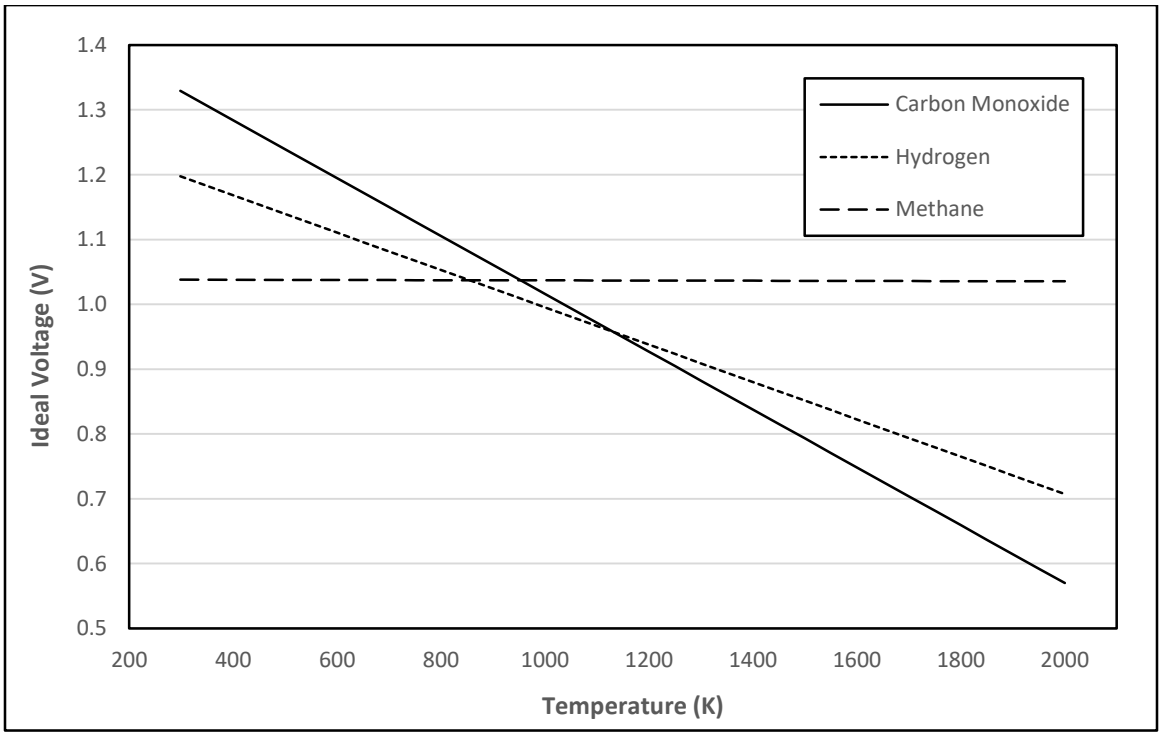

Figure 25 Ideal Voltage (V) as a function of Temperature (K) for three different fuels i.e Hydrogen, Carbon Monoxide and Methane.

We see that the Ideal Voltage is a function of Temperature for Hydrogen and Carbon Monoxide. The voltage decreases in a direct proportion with temperature. Ref [40] describes this relation as:

$$E_T = E° + \frac{\Delta S}{nF}(T - T°)$$

Where E_T is the ideal voltage at the Temperature T.

Ideal Voltage in case of Methane does not change significantly, this is because the reaction of combustion of methane results in a very low change in entropy as tabulated in APPENDIX I

6.1.3 PRESSURE DEPENDENCE OF IDEAL VOLTAGE

If p_1 is 1 atm, $R = 8.314\ kJ/kmol.K$, $F = 96485.33\ As/mol$ and
$T = 298.15\ K, 800\ K\ and\ 1073\ K$

$$\Delta E = \frac{RT}{4F} \ln\left[\frac{p_2}{p_1}\right] \quad (31)$$

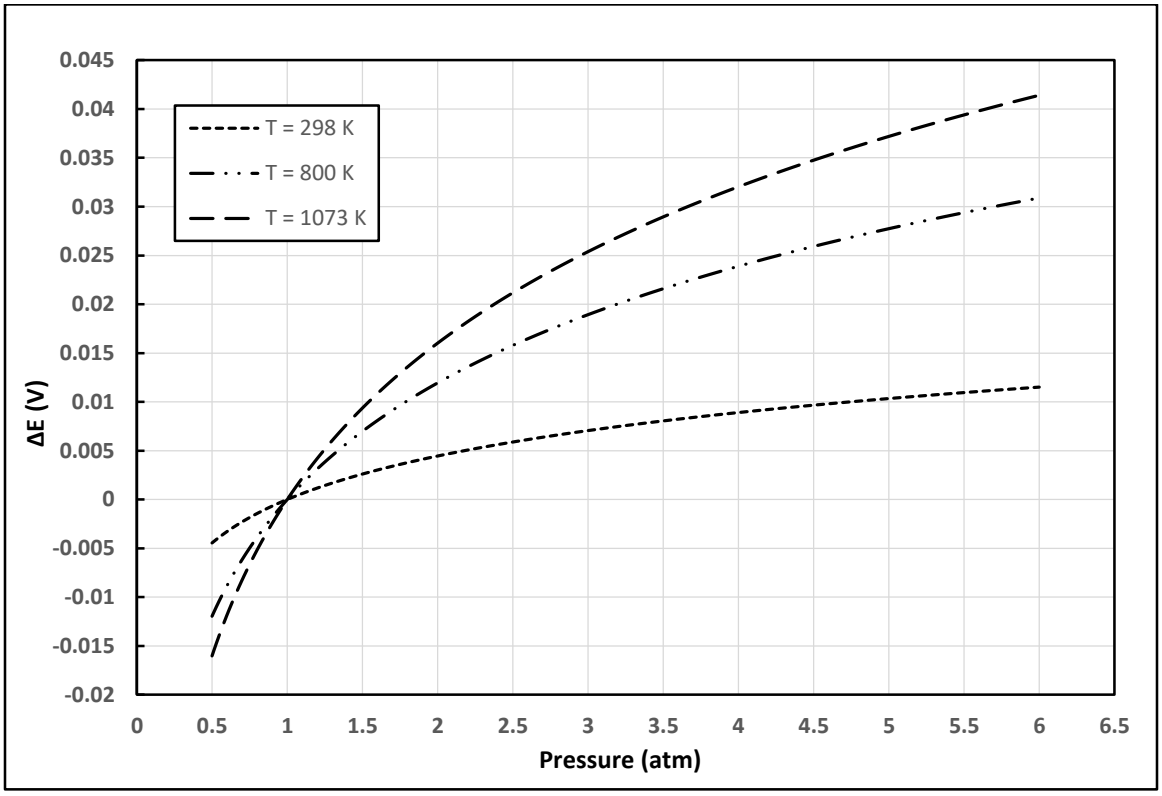

Figure 26 Increase in voltage (V) as a funcion of P2 (atm) when P1 = 1 atm for three different temperatures (K)

We see that increasing the temperature up to 6 atm at 1073 K, only increases the voltage only by 40 mV. So, therefore, pressure is only usually increased in the fuel cell to increase the voltage. Pressure can have effect on the reaction kinetics and, therefore, is increased sometimes in a fuel cell. [76]

Efficiency for three different fuels at STP is calculated in the table

Table 16 Ideal Efficiency for three different fuels at STP

Fuel	Overall Cell Reaction	η
Hydrogen	$H_2 + \frac{1}{2}O_2 \longrightarrow H_2O$	0.9453
Carbon Monoxide	$CO + \frac{1}{2}O_2 \longrightarrow CO_2$	0.9091
Methane	$CH_4 + 2O_2 \longrightarrow CO_2 + 2H_2O$	0.9982

6.2 THERMAL ANALYSIS OF A SOLID OXIDE FUEL CELL

6.2.1 RESULTS

There are regions of high stress concentration where the interconnect is attached to the air and fuel inlets. These areas need to be further strengthened. Furthermore, we analysed the fuel cell deformation and the primarily the shear stress arising in the layers. The results have been tabulated.

Table 17: Thermal Stresses induced in XZ plane in the electrodes

Cathode	Anode (MPa)	Electrolyte (MPa)	Cathode (MPa)
<u>40% Porous Ni – YSZ Anode</u>			
Porous Platinum	61.07	48.44	36.75
Zirconium Dioxide	63.80	54.04	25.33
Strontium Doped Lanthanum Manganite	25.28	21.83	13.37

26% Porous Ni – YSZ Anode			
Porous Platinum	12.59	13.55	23.19
Zirconium Dioxide	12.49	8.09	15.64
Strontium Doped Lanthanum Manganite	4.91	13.90	18.88

Table 18: Calculated Safety factors

Cathode	Anode Safety Factor	Electrolyte Safety Factor	Cathode Safety Factor
40% Porous Ni – YSZ Anode			
Porous Platinum	1.15	3.41	2.72
Zirconium Dioxide	1.10	3.05	15.79
Strontium Doped Lanthanum Manganite	2.77	7.56	6.96
26% Porous Ni – YSZ Anode			
Porous Platinum	5.56	12.18	4.31
Zirconium Dioxide	5.60	20.40	25.58
Strontium Doped Lanthanum Manganite	14.26	11.87	4.93

6.2.2 ANALYSIS

Our primary aim was to analyse the shear stress that develops between the different layers of the fuel cell. Although similar thermal stresses arise in the interconnect, they are concentrated primarily near the fuel and air inlet tubes that can be easily strengthened.

Significant shear stresses arise in the cathode, anode and electrolyte as can be clearly seen and unless we optimize our design, it is possible that our fuel cell's life is significantly reduced. The results are summarized as follows:

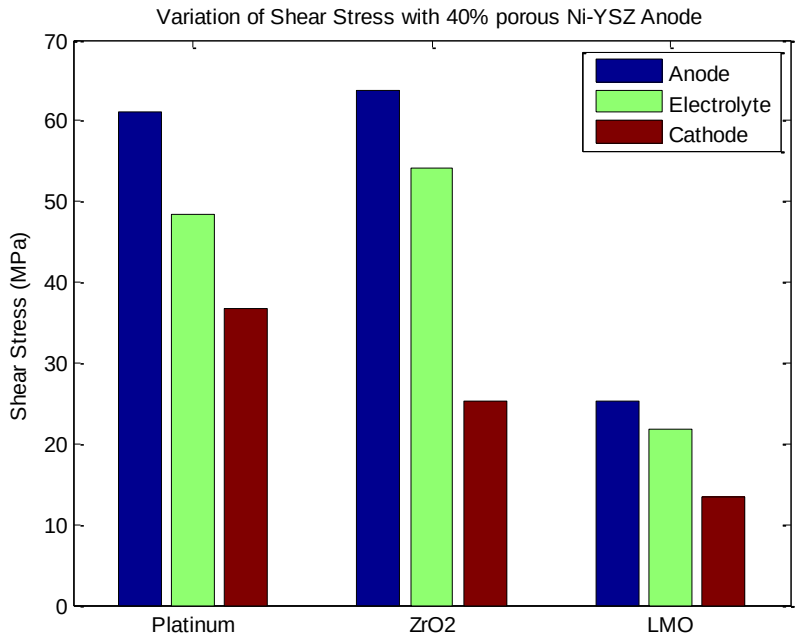

Figure 27: Shear stress with 40% porous Ni-YSZ Anode

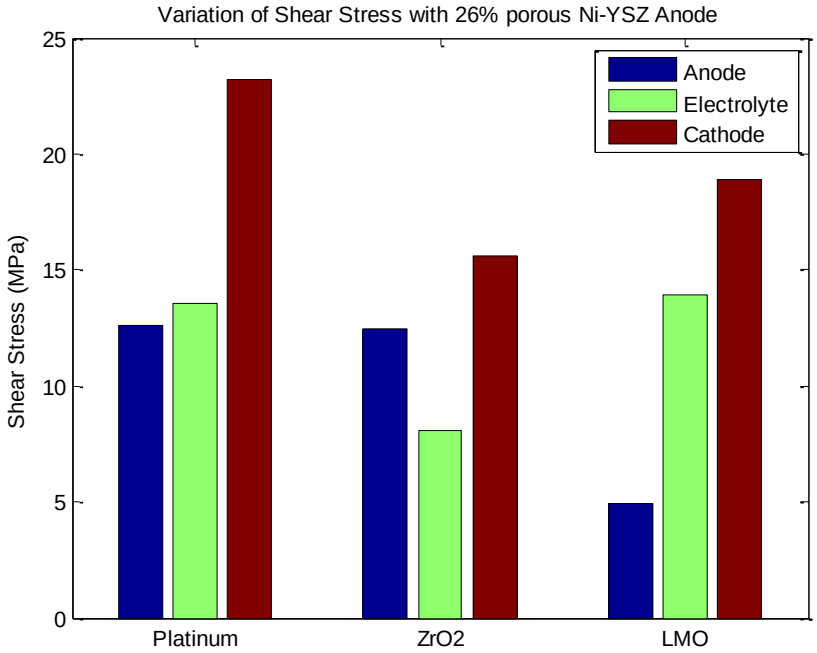

Figure 28: Shear stress with 26% porous Ni-YSZ Anode

The use of Platinum and Zirconium Dioxide results in high shear stresses. However, the use of Strontium Doped Lanthanum Manganite results in a comparatively lower shear stress between the layers of the electrode.

6.3 PERFORMANCE OF A SOLID OXIDE FUEL CELL

6.3.1 RESULTS

For the gasifier at 600C and dry air, the following results are obtained:

Table 19: Polarisation Voltage, Current Density and Power Density for 600 C Gasifier and Dry Air

Polarization Voltage (V)	Current Density (A/m^2)	Power Density (W/m^2)
0.05	458.77	435.8
0.1	838.1	754.3
0.2	1436.3	1149.5
0.3	1999.6	1399.7
0.4	2634.5	1580.7
0.5	3346.5	1674.9
0.6	4135.6	1654.3
0.7	4981.1	1494.3
0.8	5877.2	117505

For the gasifier at $800°C$ and dry air, the following results are obtained:

Table 20: Polarisation Voltage, Current Density and Power Density for 800 C Gasifier and Dry Air

Polarization Voltage (V)	Current Density (A/m^2)	Power Density (W/m^2)
0.05	586.0	556.7
0.1	1123.3	1010.9
0.2	2096.2	1677.0
0.3	3005.2	2103.7
0.4	3905.3	2343.2
0.5	4820.9	2410.5
0.6	5759.7	2303.9

0.7	6721.5	2016.4
0.8	7700.2	1540.0

For the gasifier at 1000C and dry air, the following results are obtained:

Table 21: Polarisation Voltage, Current Density and Power Density for 1000 C Gasifier and Dry Air

Polarization Voltage (V)	Current Density (A/m^2)	Power Density (W/m^2)
0.05	612.5	581.9
0.1	1177.5	1059.8
0.2	2206.0	1764.8
0.3	3167.7	2217.4
0.4	4117.3	2470.4
0.5	5079.9	2539.9
0.6	6064.2	2425.7
0.7	7067.1	2120.1
0.8	8083.3	1616.7

For the gasifier at 1000C and pure oxygen, the following results are obtained:

Table 22: Polarisation Voltage, Current Density and Power Density for 1000 C Gasifier and Pure Oxygen

Polarization Voltage (V)	Current Density (A/m^2)	Power Density (W/m^2)
0.05	675.4	641.6
0.1	1333.0	1199.7
0.2	2595.6	2076.5
0.3	3796.3	2657.4
0.4	4945.3	2967.2
0.5	6050.8	3025.4
0.6	7114.4	2845.8
0.7	8131.1	2439.3
0.8	9092.6	1818.5

The results have been graphed as follows:

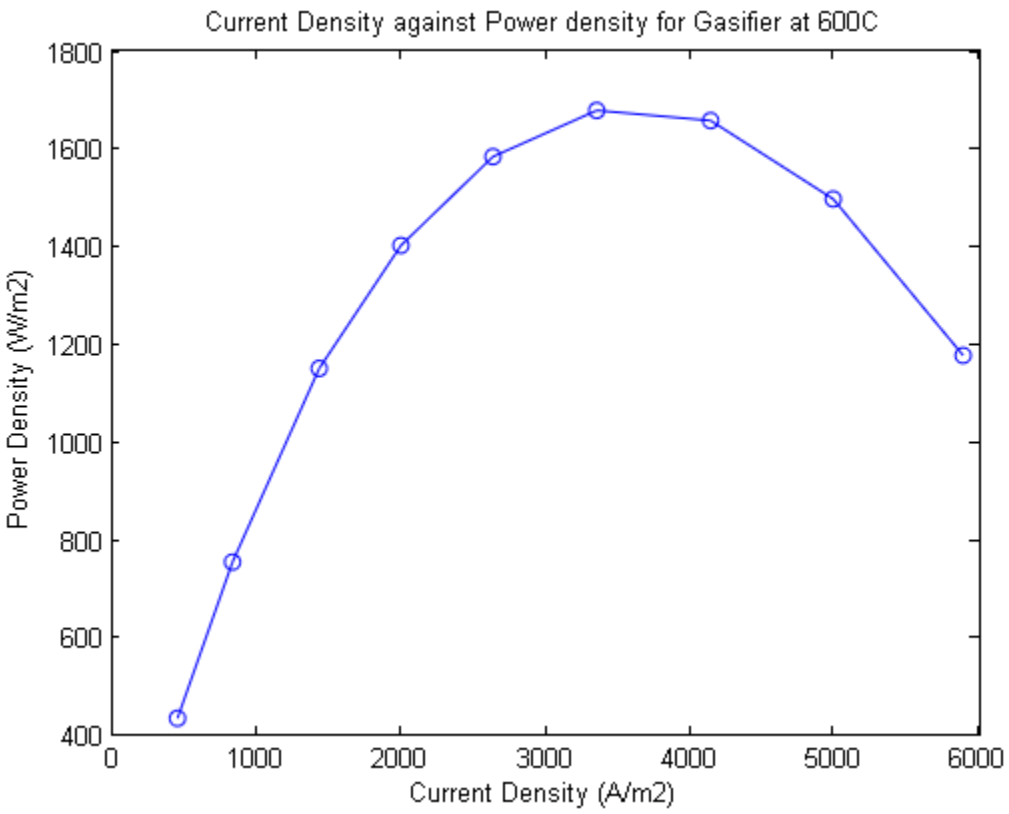

Figure 29: Current and Power Density for 600 C Gasifier Temperature

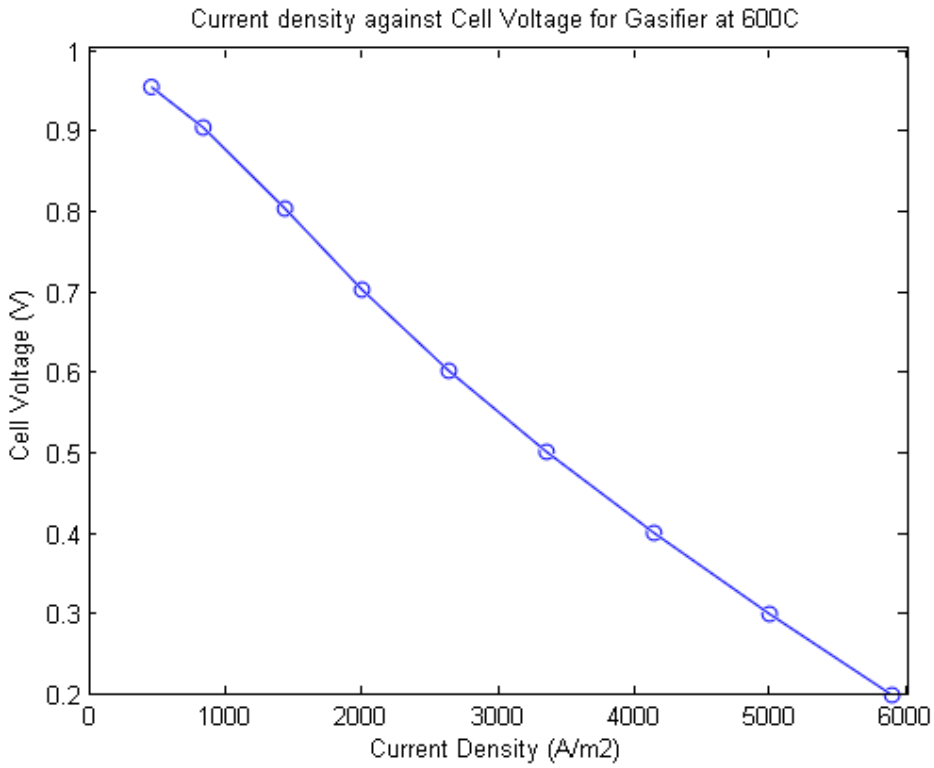

Figure 30: Voltage and Current Density for 600 C Gasifier Temperature

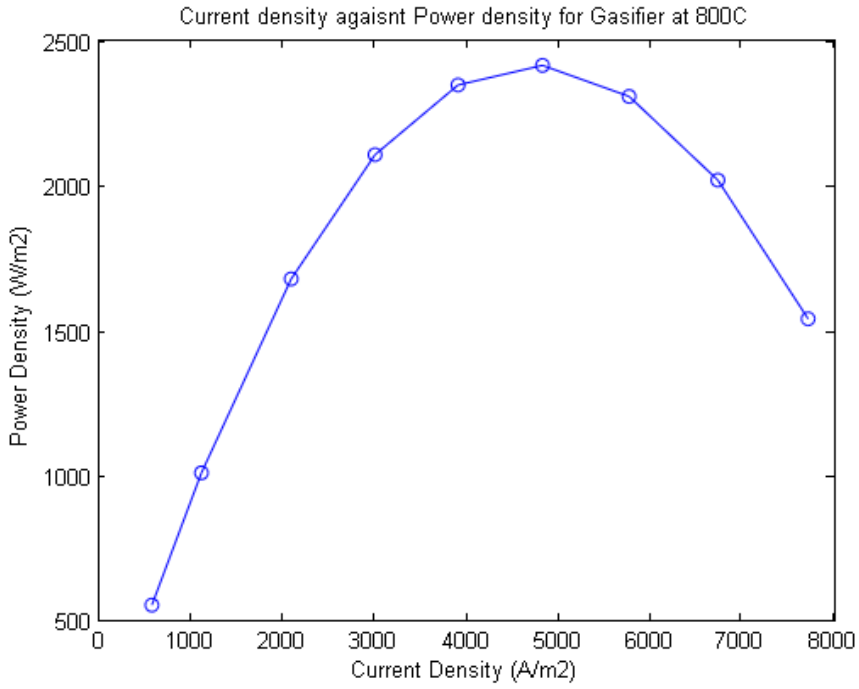

Figure 31: Current and Power Density for 800 C Gasifier Temperature

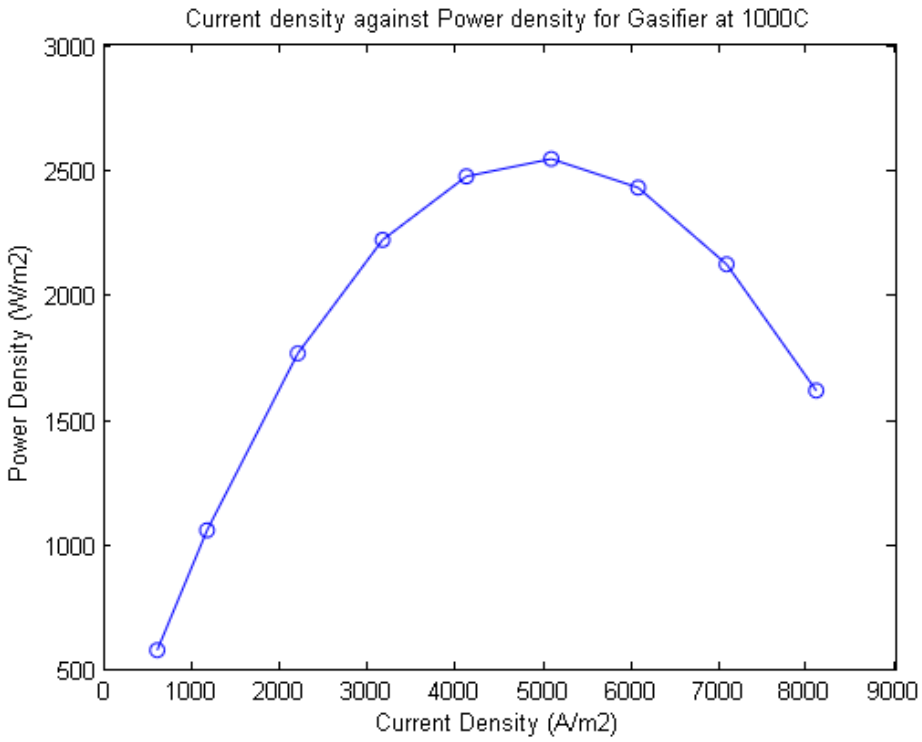

Figure 32: Current and Power Density for 1000 C Gasifier Temperature

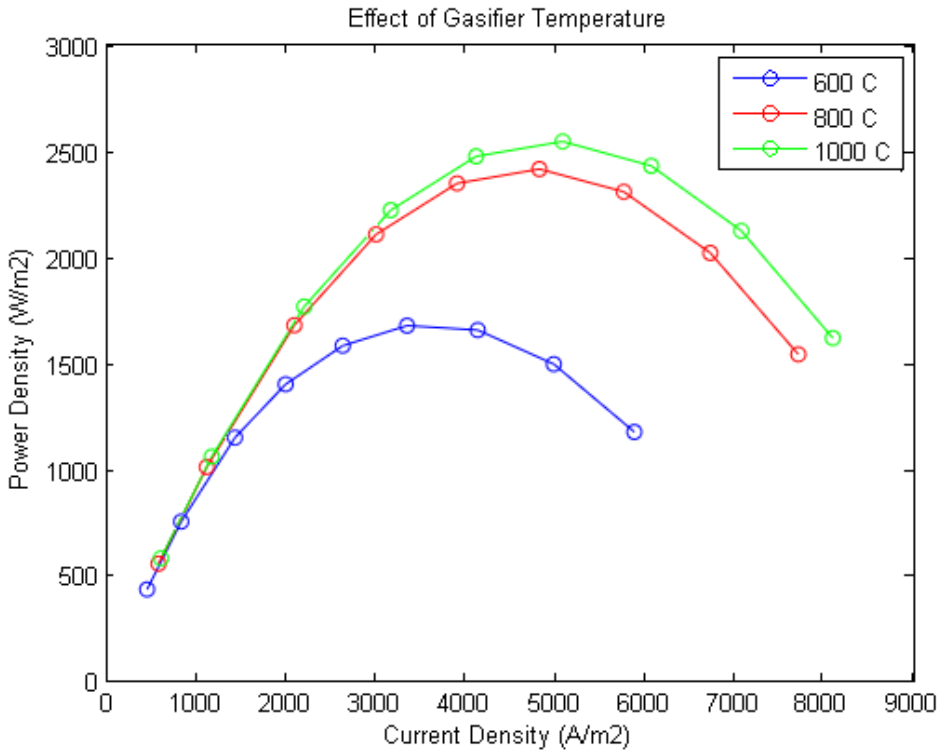

Figure 33: Effect of Gsifier Temperature on Power Density of Fuel Cell

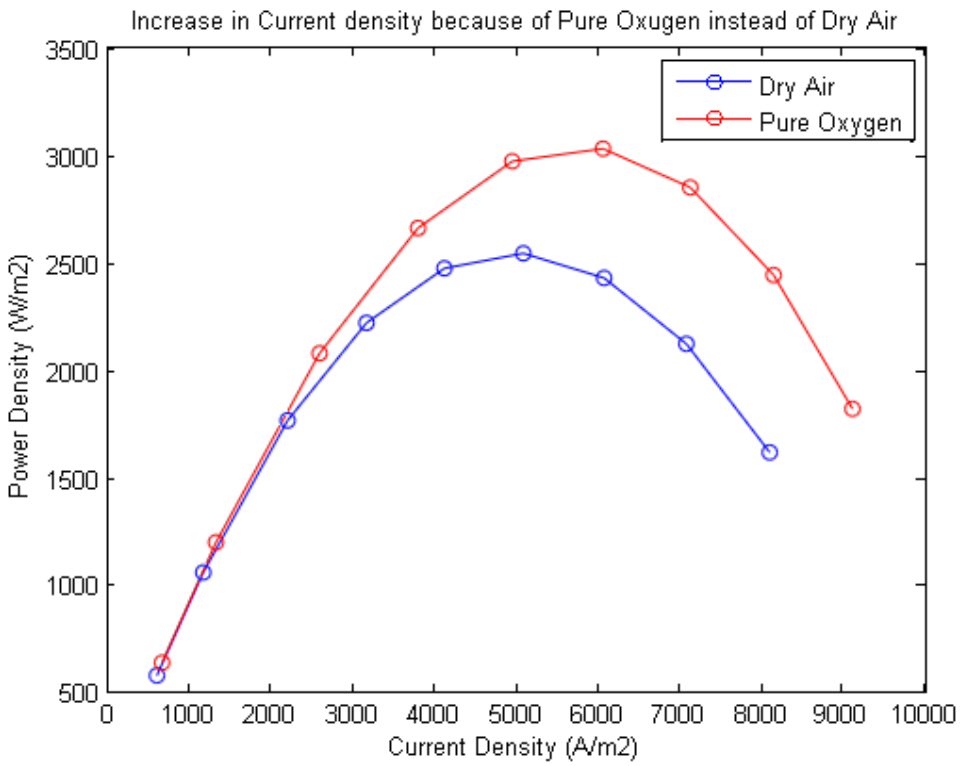

Figure 34: Effect of Oxygen Concentration on Power Density of Fuel Cell

The molar concentration of fuel changes along the length of the channel and varies as follows:

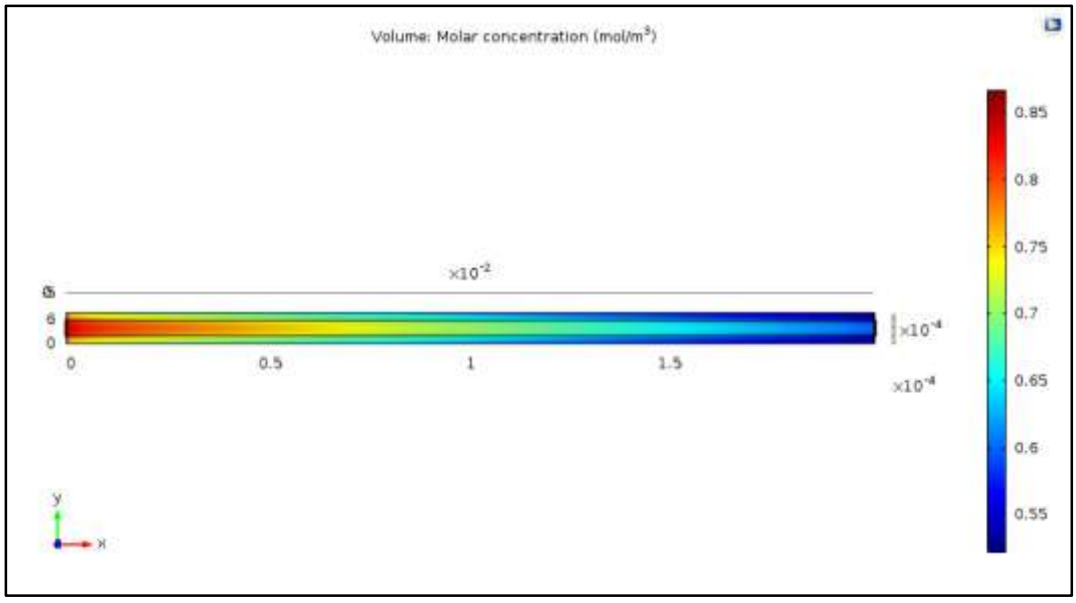

Figure 35: Carbon Monoxide molar concentration variation

Detailed results for the molar concentration are as follows:

Table 23: Inlet and Outlet CO Molar Concetration at different Gasifier Temperatures

Gasifier Temperature (C)	Inlet weight fraction of Carbon Monoxide	Inlet molar concentration (mol/m^3)	Outlet molar concentration (mol/m^3)
600	0.0512	0.89	0.40
800	0.8133	9.90	8.23
1000	0.9855	11.25	9.45

The pressure drops across the fuel channel and is essentially constant (negligible variation) as the inlet weight fraction of the carbon monoxide changes. The pressure drop for the fuel channel is as follows:

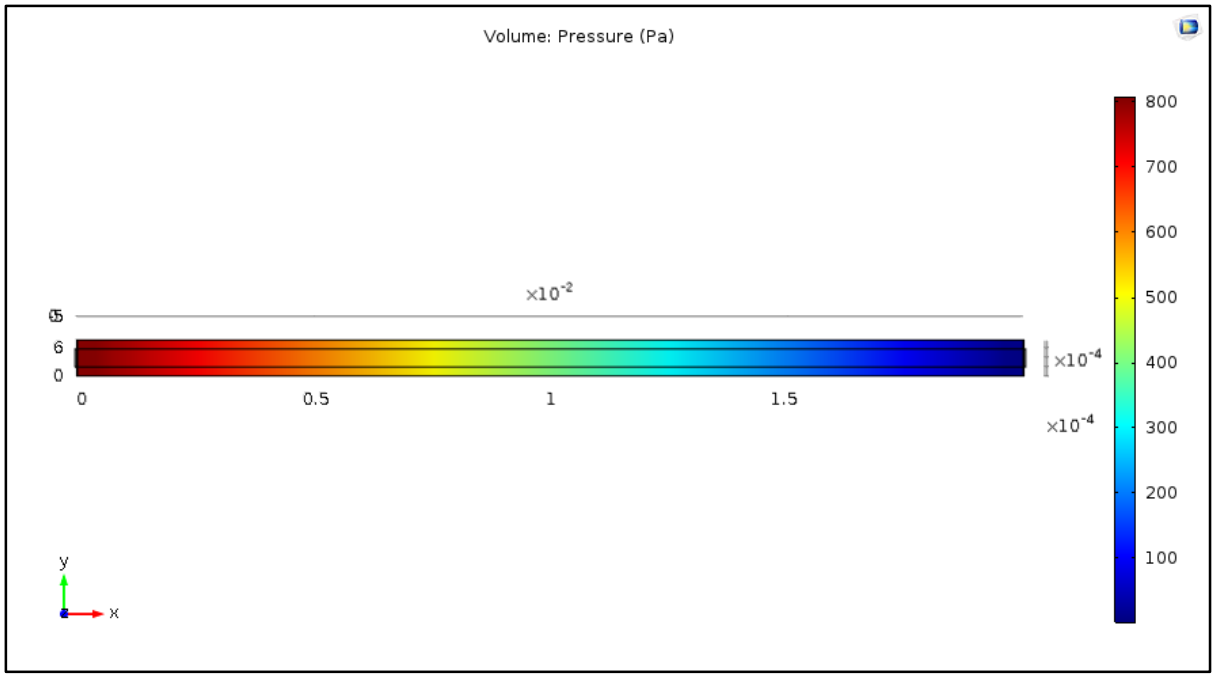

Figure 36: Pressure drop in anode channel

Similarly, the pressure drop for the oxygen channel is as follows:

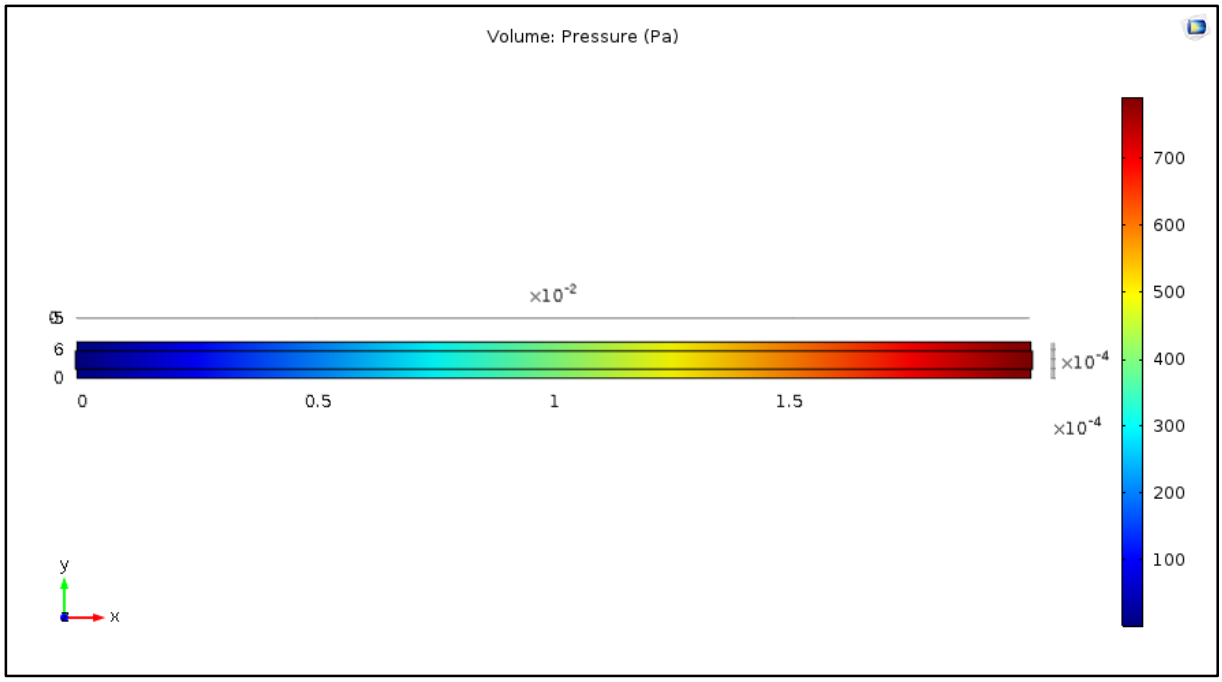

Figure 37: Pressure drop in Cathode Channel

6.3.2 DISCUSSION

As expected, more power can be extracted from our fuel cell if a higher weight fraction of carbon monoxide is provided to the anode fuel channel or if pure oxygen is supplied to the cathode fuel channel instead of dry air.

Table 24: Maximum Power obtained with Dry Air at Different Gasifier Temperatures

Gasifier Temperature (C)	Maximum Power (W/m^2)	Percentage Increase (%)
600	1674.9	0
800	2410.5	30.5
1000	2539.9	34.1

Fuel utilization, however, drops off as we increase the gasifier temperature:

Table 25: Fuel Utilisation variation with change in Gasifier Temperature

Gasifier Temperature (C)	Inlet molar concentration (mol/m^3)	Outlet molar concentration (mol/m^3)	Fuel Utilisation (%)
600	0.89	0.40	55.1
800	9.90	8.23	16.9
1000	11.25	9.45	16

6.4 EXPERIMENTAL RESULTS

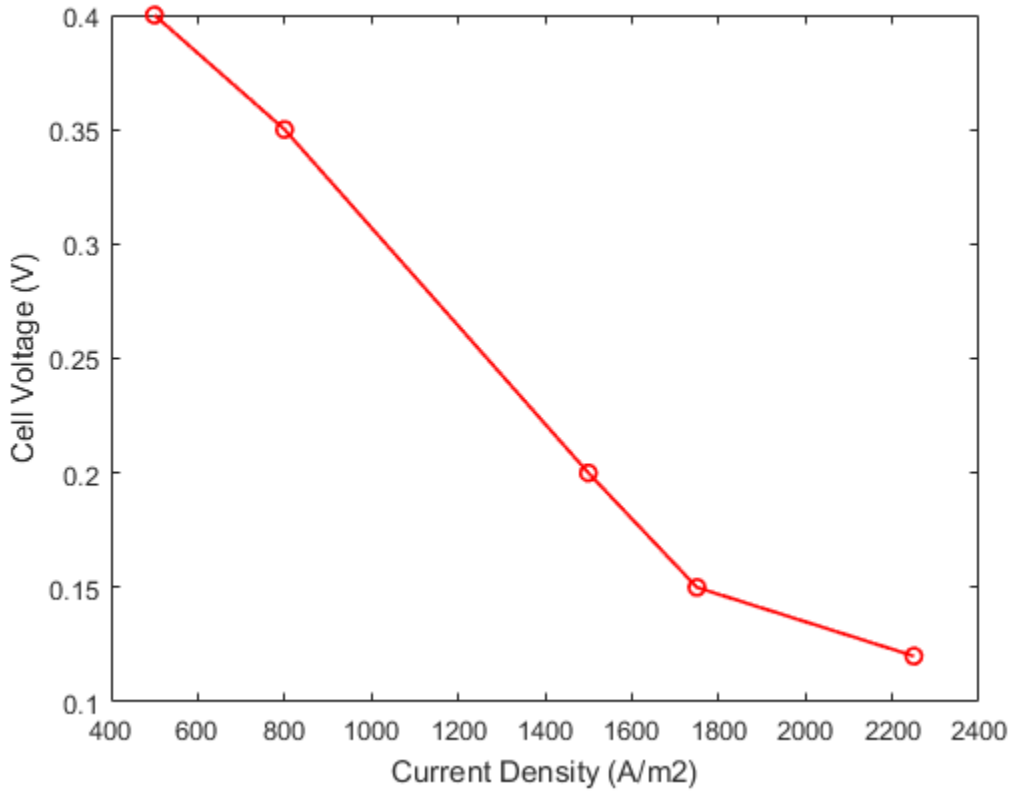

Solid Oxide Fuel Cells have the highest current and power densities of any other energy production technology. Even more so than Internal Combustion Engines and represent a revolution in the energy sector if utilized properly.

While our theoretical results demonstrated power densities ranging from 1.7 W/cm^2 to 5 W/cm^2, we were only able to extract around 2 W/cm^2 from our final fuel cell. While

nothing to be scoffed at, our fuel cell did show a slightly inferior performance than what our theoretical results had predicted. This can be due to a variety of reasons such as:

- Leakage. The surface of our dies was not completely plain and gold was not used as a sealant. The clamping force of our holder instead was relied upon as a cheaper alternative. There was slightly leakage and any such leakage does result in a drop in performance.
- Resistance of current collectors. The higher the resistance of the current collectors, the more will be the voltage drop across them and the performance of the fuel cell will degrade. Power will be dissipated across the current collectors and will therefore not be extracted as useful power.
- Primitive load cell testing equipment. The expensive nature of these load cells meant that a primitive one had to be used and accuracy had to be sacrificed.

CHAPTER 07 – CONCLUSIONS AND RECOMMENDATIONS

7.1 THERMODYNAMICS OF A FUEL CELL

7.1.1 SELECTION OF FUEL

We make use of Pugh Chart to decide which fuel is best suited to be used in a Fuel Cell

Table 26: Pugh Chart for Fuel Selection

Criteria	Weight	Baseline	CO	H	CH_4
Ideal Voltage	5	0	+	0	-
Availability	3	0	-	-	+
Amount of heat given out to sustain the temperature of a Fuel Cell	2	0	+	+	-
Storage	2	0	+	-	+
TOTAL	10		6	-3	-2

Hydrogen is not readily available. It is always produced by the electrolysis of Water. Secondly, its atoms are so small that make its storage difficult.

Carbon monoxide, like hydrogen, is not easily available but can be produced by gasification using the Reverse Boudouard Reaction. It gives the highest Ideal Voltage and is easy to store because of its large molecules.

Methane gives the lowest ideal voltage but it easily available. Most of the energy produced is utilized as electrical work and it generates no heat so the reaction cannot sustain the high temperature of an SOFC.

Therefore, Carbon Monoxide is the most ideal fuel to be used in an SOFC.

7.1.2 EFFICIENCY COMPARISON OF A FUEL CELL AND A CARNOT ENGINE

The reversible thermal efficiency of a fuel cell is given by:

$$\eta = \frac{\Delta G}{\Delta H}$$

The efficiency of a Carnot Engine is given by:

$$\eta = 1 - \frac{T_L}{T_H}$$

If we assume the Low Temperature reservoir to be at 298.15 K, the efficiency of a Fuel Cell and Carnot Engine can be compared in the following graph.

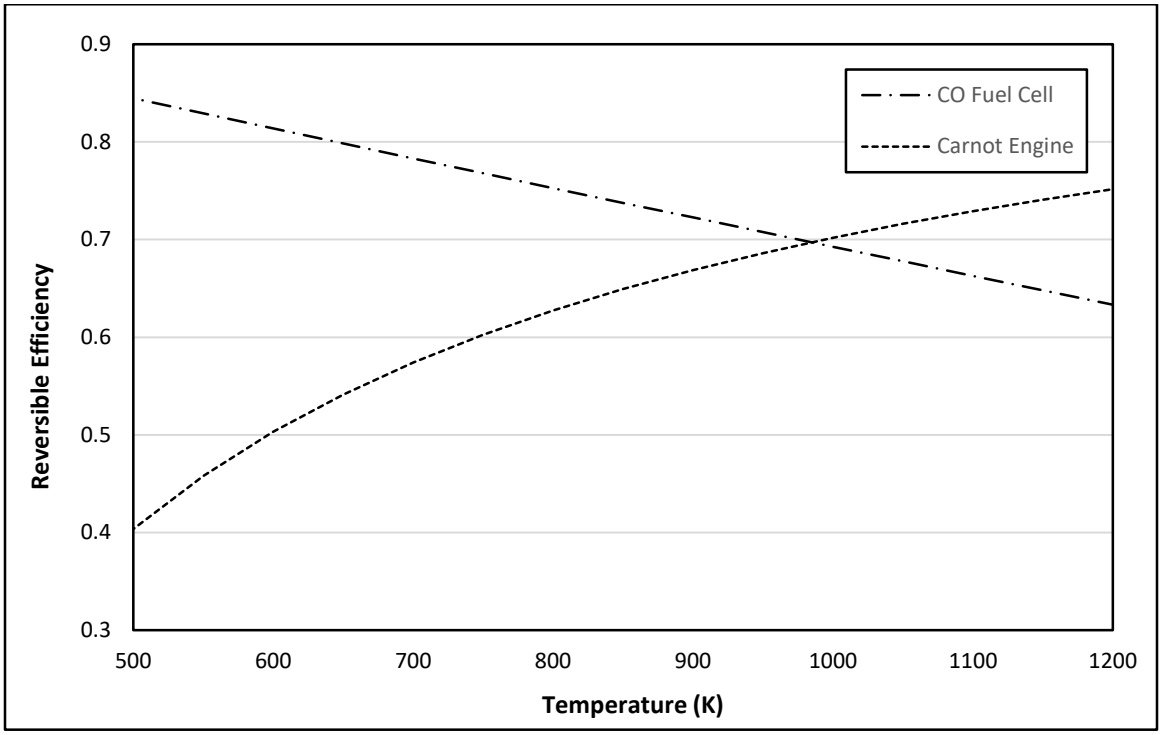

Figure 38 A comparison of Carbon Monoxide fueled Fuel Cell efficiency and Carnot Engine Efficiency

7.2 THERMAL ANALYSIS OF A SOLID OXIDE FUEL CELL

In order to decide the most effective cathode material for our fuel cell, we utilize a Pugh chart as follows:

Criteria	Weight	Baseline	Porous Platinum	Zirconium Dioxide	Strontium Doped Lanthanum Manganite
Thermal Properties	5	0	0	-	+
Resistance to Shear Failure	3	0	0	+	-

Cost	3	0	-	-	+
Availability	3	0	-	-	-
Ease of Manufacture	2	0	-	+	0
Total		0	-8	-6	2

Table 27: Pugh Chart for Material Selection

Strontium Doped Lanthanum Manganite therefore provides the best mix of properties despite its inferior resistance to shear failure.

7.3 PERFORMANCE OF A SOLID OXIDE FUEL CELL

While the higher gasifier temperatures do offer significantly higher power, the fuel utilization drops off sharply. Despite the fact that the actual fuel utilization will be higher because of the several closely spaced paths that the gas will be routed through, the added cost of maintaining the gasifier at a higher temperature is another issue that needs to be addressed.

There is a 30.5% increase in the maximum power that we are obtaining if we increase the gasifier temperature from 600 to 800 Celsius. There is only a very marginal increase in maximum power, however, if we increase the gasifier temperature further beyond the point. That, coupled with the lower fuel utilization and the added energy costs means that maintaining the gasifier at a temperature higher than 800 Celsius is impractical.

7.4 FUTURE RECOMMENDATIONS

Fuel cells suffer from two main drawbacks that are rendering them unviable for everyday electricity generation. One of the problems is to be able to stack fuel cells while preventing leakage. While it is relatively simple and straightforward to seal fuel cells if a single cell is used, it becomes progressively difficult to seal them if multiple cells are stacked on top of each other. Gold is often used which is expensive and is therefore not a feasible or viable method of sealing fuel cells.

The other problem is the difficulty of manufacturing large fuel cells. Button fuel cells with a diameter of 10 to 13 mm are easy to make but they produce little power and are not viable for mass scale energy production. Larger fuel cells are difficult to handle in the production stage are may break down because of their brittle nature. Future work must be done to be able to produce large fuel cells in a cheap and efficient manner in order to make them viable.

Similarly, for gasification, future work can be done on how the gasification process can be used for carbon capture from organic waste. By doing so, we can not only help reduce the waste in landfills, but also help bridge the gap between energy demand and energy supply.

APPENDIX I: PROPERTIES OF REACTIONS OF HYDROGEN, CARBON MONOXIDE AND METHANE

HYDROGEN

$$H_2 + \frac{1}{2}O_2 \longrightarrow H_2O$$

Number of electrons participating = 2

T (K)	ΔH $kJ/kmol$	ΔS $kJ/kmol.K$	ΔG $kJ/kmol$	$E_{\Delta H}$ (V)	E (V)	η
298.15	-241834	-44.365	-228607	1.2532	1.1847	0.9453
500	-243834	-49.495	-219086	1.2636	1.1353	0.8985
550	-244306	-50.396	-216588	1.2660	1.1224	0.8865
600	-244766	-51.196	-214048	1.2684	1.1092	0.8745
650	-245210	-51.908	-211470	1.2707	1.0959	0.8624
700	-245640	-52.544	-208859	1.2729	1.0823	0.8503
750	-246053	-53.115	-206217	1.2751	1.0686	0.8381
800	-246450	-53.627	-203548	1.2771	1.0548	0.8259
850	-246830	-54.088	-200855	1.2791	1.0409	0.8137
900	-247193	-54.503	-198140	1.2810	1.0268	0.8016
950	-247538	-54.877	-195405	1.2828	1.0126	0.7894
1000	-247866	-55.213	-192653	1.2845	0.9984	0.7772
1050	-248176	-55.516	-189885	1.2861	0.9840	0.7651
1100	-248469	-55.788	-187102	1.2876	0.9696	0.7530
1150	-248746	-56.035	-184306	1.2890	0.9551	0.7409
1200	-249008	-56.257	-181499	1.2904	0.9406	0.7289
1250	-249254	-56.458	-178681	1.2917	0.9259	0.7169
1300	-249485	-56.639	-175853	1.2929	0.9113	0.7049
1350	-249701	-56.803	-173017	1.2940	0.8966	0.6929
1400	-249904	-56.951	-170173	1.2950	0.8819	0.6810
1450	-250095	-57.084	-167323	1.2960	0.8671	0.6690
1500	-250274	-57.206	-164465	1.2970	0.8523	0.6571

CARBON MONOXIDE

$$CO + \frac{1}{2}O_2 \longrightarrow CO_2$$

Number of electrons participating = 2

T (K)	ΔH $kJ/kmol$	ΔS $kJ/kmol.K$	ΔG $kJ/kmol$	$E_{\Delta H}$ (V)	E (V)	η
298.15	-282995	-86.267	-257274	1.4665	1.3332	0.9091
500	-283663	-88.113	-239607	1.4700	1.2417	0.8447
550	-283677	-88.139	-235200	1.4701	1.2188	0.8291
600	-283651	-88.095	-230794	1.4699	1.1960	0.8137
650	-283594	-88.004	-226392	1.4696	1.1732	0.7983
700	-283510	-87.879	-221994	1.4692	1.1504	0.7830
750	-283404	-87.733	-217604	1.4686	1.1277	0.7678
800	-283278	-87.571	-213221	1.4680	1.1049	0.7527
850	-283137	-87.4	-208847	1.4673	1.0823	0.7376
900	-282982	-87.223	-204482	1.4664	1.0597	0.7226
950	-282814	-87.041	-200125	1.4656	1.0371	0.7076
1000	-282635	-86.857	-195777	1.4647	1.0145	0.6927
1050	-282446	-86.673	-191439	1.4637	0.9921	0.6778
1100	-282249	-86.49	-187110	1.4627	0.9696	0.6629
1150	-282044	-86.308	-182790	1.4616	0.9472	0.6481
1200	-281832	-86.127	-178479	1.4605	0.9249	0.6333
1250	-281613	-85.948	-174177	1.4594	0.9026	0.6185
1300	-281388	-85.772	-169884	1.4582	0.8804	0.6037
1350	-281158	-85.599	-165600	1.4570	0.8582	0.5890
1400	-280923	-85.428	-161325	1.4558	0.8360	0.5743
1450	-280684	-85.26	-157057	1.4545	0.8139	0.5596
1500	-280440	-85.095	-152799	1.4533	0.7918	0.5449

METHANE

$$CH_4 + 2O_2 \longrightarrow CO_2 + 2H_2O$$

Number of electrons participating = 8

T (K)	ΔH $kJ/kmol$	ΔS $kJ/kmol.K$	ΔG $kJ/kmol$	$E_{\Delta H}$ (V)	E (V)	η
298.15	-802317	-4.973	-800834	1.0394	1.0375	0.9982
500	-800534	-0.328	-800370	1.0371	1.0369	0.9998
550	-800242	0.229	-800368	1.0367	1.0369	1.0002
600	-800024	0.609	-800390	1.0365	1.0369	1.0005
650	-799880	0.841	-800427	1.0363	1.0370	1.0007
700	-799805	0.952	-800472	1.0362	1.0370	1.0008
750	-799796	0.966	-800520	1.0362	1.0371	1.0009
800	-799845	0.903	-800567	1.0362	1.0372	1.0009
850	-799948	0.779	-800610	1.0364	1.0372	1.0008
900	-800097	0.608	-800644	1.0366	1.0373	1.0007
950	-800285	0.405	-800670	1.0368	1.0373	1.0005
1000	-800507	0.178	-800684	1.0371	1.0373	1.0002
1050	-800756	-0.066	-800687	1.0374	1.0373	0.9999
1100	-801030	-0.32	-800678	1.0378	1.0373	0.9996
1150	-801324	-0.582	-800655	1.0381	1.0373	0.9992
1200	-801634	-0.846	-800619	1.0385	1.0372	0.9987
1250	-801957	-1.109	-800571	1.0390	1.0372	0.9983
1300	-802290	-1.37	-800509	1.0394	1.0371	0.9978
1350	-802630	-1.627	-800434	1.0398	1.0370	0.9973
1400	-802975	-1.878	-800346	1.0403	1.0369	0.9967
1450	-803324	-2.123	-800246	1.0407	1.0367	0.9962
1500	-803675	-2.361	-800134	1.0412	1.0366	0.9956

APPENDIX II: PROPERTIES OF AIR AS A FUNCTION OF TEMPERATURE AT 1 ATMOSPHERE PRESSURE

Temperature (*K*)	Specific Heat		Ratio of Specific Heats - *k* - (c_p/c_v)	Dynamic Viscosity - μ - (10^{-5} *kg/m s*)	Thermal Conductivity (10^{-5} *kW/m K*)	Prandtl Number	Kinematic Viscosity - ν - (10^{-5} m^2/s)	Density - ρ - (kg/m^3)
	- c_p - *(kJ/kgK)*	- c_v - *(kJ/kgK)*						
175	1.0023	0.7152	1.401	1.182	1.593	0.744	0.586	2.017
200	1.0025	0.7154	1.401	1.329	1.809	0.736	0.753	1.765
225	1.0027	0.7156	1.401	1.467	2.020	0.728	0.935	1.569
250	1.0031	0.7160	1.401	1.599	2.227	0.720	1.132	1.412
275	1.0038	0.7167	1.401	1.725	2.428	0.713	1.343	1.284
300	1.0049	0.7178	1.400	1.846	2.624	0.707	1.568	1.177
325	1.0063	0.7192	1.400	1.962	2.816	0.701	1.807	1.086
350	1.0082	0.7211	1.398	2.075	3.003	0.697	2.056	1.009
375	1.0106	0.7235	1.397	2.181	3.186	0.692	2.317	0.9413
400	1.0135	0.7264	1.395	2.286	3.365	0.688	2.591	0.8824
450	1.0206	0.7335	1.391	2.485	3.710	0.684	3.168	0.7844
500	1.0295	0.7424	1.387	2.670	4.041	0.680	3.782	0.7060
550	1.0398	0.7527	1.381	2.849	4.357	0.680	4.439	0.6418
600	1.0511	0.7640	1.376	3.017	4.661	0.680	5.128	0.5883
650	1.0629	0.7758	1.370	3.178	4.954	0.682	5.853	0.5430
700	1.0750	0.7879	1.364	3.332	5.236	0.684	6.607	0.5043
750	1.0870	0.7999	1.359	3.482	5.509	0.687	7.399	0.4706
800	1.0987	0.8116	1.354	3.624	5.774	0.690	8.214	0.4412
850	1.1101	0.8230	1.349	3.763	6.030	0.693	9.061	0.4153
900	1.1209	0.8338	1.344	3.897	6.276	0.696	9.936	0.3922
950	1.1313	0.8442	1.340	4.026	6.520	0.699	10.83	0.3716
1000	1.1411	0.8540	1.336	4.153	6.754	0.702	11.76	0.3530
1050	1.1502	0.8631	1.333	4.276	6.985	0.704	12.72	0.3362
1100	1.1589	0.8718	1.329	4.396	7.209	0.707	13.70	0.3209
1150	1.1670	0.8799	1.326	4.511	7.427	0.709	14.70	0.3069
1200	1.1746	0.8875	1.323	4.626	7.640	0.711	15.73	0.2941
1250	1.1817	0.8946	1.321	4.736	7.849	0.713	16.77	0.2824
1300	1.1884	0.9013	1.319	4.846	8.054	0.715	17.85	0.2715

APPENDIX III: REACTION CONSTANTS AND WEIGHT FRACTIONS

Gasifier Temperature	Reaction Coefficient Reverse Boudouard	Carbon Monoxide Weight Fraction	Reaction Coefficient Forward Boudouard	Carbon Dioxide Weight Fraction
500	0.003949	0.002507	253.2257	0.997494
510	0.005563	0.003527	179.7718	0.996473
520	0.007767	0.004918	128.7491	0.995082
530	0.010754	0.006797	92.98944	0.993203
540	0.014769	0.009311	67.71025	0.990689
550	0.020124	0.012644	49.69102	0.987356
560	0.027216	0.017024	36.74358	0.982976
570	0.036539	0.022723	27.36833	0.977277
580	0.048712	0.030066	20.52898	0.969934
590	0.064501	0.039428	15.5036	0.960572
600	0.084851	0.05123	11.78535	0.94877
610	0.110917	0.06593	9.015719	0.93407
620	0.144107	0.084001	6.939277	0.915999
630	0.186125	0.1059	5.372737	0.8941
640	0.239023	0.132024	4.183697	0.867976
650	0.305262	0.16266	3.275875	0.83734
660	0.387775	0.197925	2.578812	0.802075
670	0.490046	0.237716	2.040625	0.762284
680	0.616187	0.281671	1.622883	0.718329
690	0.771039	0.329157	1.296952	0.670843
700	0.960268	0.379298	1.041376	0.620702
710	1.190484	0.431036	0.839994	0.568964

720	1.469366	0.483218	0.680566	0.516782
730	1.805797	0.534698	0.553772	0.465302
740	2.210019	0.584437	0.452485	0.415563
750	2.693792	0.631572	0.371224	0.368428
760	3.270578	0.675459	0.305756	0.324541
770	3.955725	0.715689	0.252798	0.284311
780	4.766684	0.752067	0.209789	0.247933
790	5.723222	0.784578	0.174727	0.215422
800	6.847668	0.813349	0.146035	0.186651
810	8.165162	0.838606	0.122472	0.161394
820	9.703927	0.860632	0.103051	0.139368
830	11.49556	0.879741	0.08699	0.120259
840	13.57532	0.896253	0.073663	0.103747
850	15.98247	0.91048	0.062569	0.08952
860	18.7606	0.922712	0.053303	0.077288
870	21.95799	0.933214	0.045541	0.066786
880	25.62797	0.942226	0.03902	0.057774
890	29.82928	0.949956	0.033524	0.050044
900	34.62654	0.956588	0.02888	0.043412
910	40.09061	0.962282	0.024943	0.037718
920	46.29903	0.967173	0.021599	0.032827
930	53.33647	0.971381	0.018749	0.028619
940	61.2952	0.975004	0.016314	0.024996
950	70.27556	0.978128	0.01423	0.021872
960	80.38642	0.980826	0.01244	0.019174
970	91.7457	0.98316	0.0109	0.01684
980	104.4809	0.985183	0.009571	0.014817
990	118.7294	0.986938	0.008423	0.013062
1000	134.6395	0.988463	0.007427	0.011537

1010	152.3703	0.989792	0.006563	0.010208
1020	172.0927	0.990951	0.005811	0.009049
1030	193.9898	0.991965	0.005155	0.008035
1040	218.2573	0.992852	0.004582	0.007148
1050	245.1043	0.99363	0.00408	0.00637
1060	274.7538	0.994313	0.00364	0.005687
1070	307.4429	0.994915	0.003253	0.005085
1080	343.4238	0.995445	0.002912	0.004555
1090	382.9643	0.995913	0.002611	0.004087
1100	426.3479	0.996328	0.002346	0.003672
1110	473.8747	0.996695	0.00211	0.003305
1120	525.862	0.997021	0.001902	0.002979
1130	582.6446	0.99731	0.001716	0.00269
1140	644.5752	0.997568	0.001551	0.002432
1150	712.0252	0.997798	0.001404	0.002202
1160	785.3851	0.998003	0.001273	0.001997
1170	865.0648	0.998187	0.001156	0.001813
1180	951.4943	0.998351	0.001051	0.001649
1190	1045.124	0.998499	0.000957	0.001501
1200	1146.424	0.998631	0.000872	0.001369

BIBLIOGRAPHY

1. Ormerod, R.M., *Solid oxide fuel cells.* Chemical Society Reviews, 2003: p. 17-28.
2. Dicks, A.L., *Molten carbonate fuel cells.* Current Opinion in Solid State and Material Science, 2004: p. 379-383.
3. Kamarudin, S.K., F. Achmad, and W.R.W. Daud, *Overview on the application of direct methanol fuel cell.* International Journal of Hydrogen Energy, 2009.
4. McLean, G.F., et al., *An assessment of alkaline fuel cell technology.* International Journal of Hydrogen Energy 2002: p. 507-526.
5. Sammes, N., R. Bove, and K. Stahl, *Phosphoricacid fuel cells: Fundamentals and applications.* Current Opinion in Solid State and Materials Science, 2004: p. 372-378.
6. Wang, Y., et al., *A review of polymer electrolyte membrane fuel cells: technology, applications, and needs on fundamental research.* Applied energy, 2011. 88(4): p. 981-1007.
7. Clarke, S.H., et al., *Catalytic aspects of the steam reforming of hydrocarbons in internal reforming fuel cells.* Catalysis Today, 1997: p. 411-423.
8. Hao, Y. and D.G. Goodwin, *Numerical study of heterogeneous reactions in an SOFC anode with oxygen addition.* Journal of the Electrochemical Society, 2008: p. 666-674.
9. *World Energy Resources: Coal*. 2013.
10. *World Energy Resources: Coal*. 2016.
11. Shafiee, S. and E. Topal, *When will fossil fuel reserves be diminished?* Energy Policy, 2009: p. 181-189.
12. Pakistan, M.o.P.a.N.R.-G.o., *Coal Resources of Pakistan - An Overview*. 2015.
13. *Upgrading the Efficiency of the World's Coal Fleet to Reduce CO2 Emissions.* Cornerstone-The Official Journal of the World Coal Industry, 2015.
14. Cao, D., Y. Sun, and G. Wang, *Direct carbon fuel cell: Fundamentals and recent developments.* Journal of Power Sources, 2007: p. 250-257.
15. Giddey, S., et al., *A comprehensive review of direct carbon fuel cell technology.* Progress in Energy and Combustion Science, 2012: p. 360-399.

16. Blomen, L. JMJ, and M.N. Mugerwa, *Fuel cell systems: History*, in *Springer Science & Business Media*. 2013.
17. *The fuel cell industry review.* Fuel Cell Today, 2013.
18. Ellis, M.W., M.R.V. Spakovsky, and D.J. Nelson. *Fuel cell systems: efficient, flexible energy conversion for the 21st century*. in *Proceedings of the IEEE*. 2001.
19. *EG&G technical services*, in *Handbook, Fuel Cell*. 2004. p. 1-10.
20. Dhathathreyan, K.S. and N. Rajalakshmi, *Polymer Electrolyte Membrane Fuel Cell.* Recent trends in fuel cell science and technology, 2007: p. 40-115.
21. Sopian, K. and W.R.W. Daud, *Challenges and future developments in proton exchange.* Renewable Energy 2006: p. 719-727.
22. McGrath, et al., *Direct methanol fuel cells.* Journal of Industrial and Engineering Chemistry 2004: p. 1063-1080.
23. Hogarth, M.F. and G.A. Hards, *Direct methanol fuel cells.* Platinum Metals Review, 1996: p. 150-159.
24. Sotuchi, H., *ENERGY CARRIERS AND CONVERSION SYSTEMS.* ALKALINE FUEL CELLS. 2.
25. E, P., et al., *The influence of Pt on the electrooxidation behavior of carbon in phosphoric acid.* Electrochimica, 1992.
26. Bischoff, M., *Molten carbonate fuel cells: A high temperature fuel cell on the edge to commercialization.* Journal of Power Sources 2006: p. 842-845.
27. Plomp, L., et al., *Improvement of molten-carbonate fuel cell (MCFC) lifetime.* Journal of power sources, 1992: p. 369-373.
28. Appleby, A.J. and F.R. Foulkes, *Fuel cell handbook*. 1988: New York, NY; Van Nostrand Reinhold Co. Inc.
29. Yang, Z., et al., *Electrical contacts between cathodes and metallic interconnects in solid oxide fuel cells.* Journal of Power Sources, 2006: p. 246-252.
30. Zuo, C., M. Liu, and M. Liu, *Solid Oxide Fuel Cells.* Sol-Gel Processing for Conventional and Alternative Energy, 2012: p. 7-36.
31. Gellings, P.J. and H.J. Bouwmeester., *Advantages and drawbacks of solid oxide fuel cells*, in *Handbook of solid state electrochemistry*. 1997, CRC Press. p. 408.

32. Selcuk, A., G. Merere, and A. Atkinson, *cells., The influence of electrodes on the strength of planar zirconia solid oxide fuel.* Journal of Materials Science, 2001: p. 1173-1182.
33. Montross, C.S., H. Yokokawa, and M. Dokiya, *Thermal stresses in planar solid oxide fuel cells due to thermal expansion differences.* British Ceramic Transactions, 2002: p. 85-93.
34. H.Yakabe, et al., *Evaluation of residual stresses in a SOFC stack.* Journal of power sources 2004: p. 278-284.
35. H., Y., et al., *Evaluation of the residual stress for anode-supported SOFCs.* Journal of Power Sources, 2004: p. 9-16.
36. Fischer, W., et al., *Residual stresses in planar solid oxide fuel cells.* Journal of Power Sources, 2005: p. 73-77.
37. Yakabe, H., et al., *3-D model calculation for planar SOFC.* Journal of power sources, 2001: p. 144-154.
38. Selimovic, A., et al., *Steady state and transient thermal stress analysis in planar solid oxide fuel cells.* Journal of Power Sources, 2005: p. 463-469.
39. Nakajo, A., et al., *Modeling of thermal stresses and probability of survival of tubular SOFC.* Journal of Power Sources, 2006: p. 287-294.
40. O'hayre, R., et al., *Fuel cell fundamentals*. 2016: John Wiley & Sons.
41. Cimenti, M. and J. Hill, *Thermodynamic analysis of solid oxide fuel cells operated with methanol and ethanol under direct utilization, steam reforming, dry reforming or partial oxidation conditions.* Journal of Power Sources, 2009. 186(2): p. 377-384.
42. Hirschenhofer, J., et al., *The fuel cell handbook, 4th.* Reading, PA: Parsons Corporation, 1998.
43. Smith, J.M., H.C. Van Ness, and M.M. Abbott, *Introduction to Chemical Engineering Thermodynamics*. 1996.
44. Cengel, Y.A. and M.A. Boles, *Thermodynamics: an engineering approach.* Sea, 2002. 1000: p. 8862.
45. Stull, D.R. and H. Prophet, *JANAF thermochemical tables*. 1971, National Standard Reference Data System.

46. Handbook, F.C., *EG&G technical services.* Inc., Albuquerque, NM, DOE/NETL-2004/1206, 2004: p. 1-10.
47. Prausnitz, J.M., R.N. Lichtenthaler, and E.G. de Azevedo, *Molecular thermodynamics of fluid-phase equilibria*. 1998: Pearson Education.
48. Moran, M.J., et al., *Fundamentals of engineering thermodynamics*. 2010: John Wiley & Sons.
49. Zoski, C.G., *Handbook of electrochemistry*. 2006: Elsevier.
50. Hemmes, K., M. Houwing, and N. Woudstra, *Modeling of a direct carbon fuel cell system.* Journal of Fuel Cell Science and Technology, 2010. 7(5): p. 051008.
51. Larminie, J., A. Dicks, and M.S. McDonald, *Fuel cell systems explained*. Vol. 2. 2003: J. Wiley Chichester, UK.
52. Appleby, A.J., *Fuel cell handbook.* 1988.
53. Selcuk, A., G. Merere, and A. Atkinson, *The influence of electrodes on the strength of planar zirconia solid oxide fuel cells.* Journal of Materials Science, 2001. 36(5): p. 1173-1182.
54. Montross, C., H. Yokokawa, and M. Dokiya, *Thermal stresses in planar solid oxide fuel cells due to thermal expansion differences.* British Ceramic Transactions, 2002. 101(3): p. 85-93.
55. Yakabe, H., et al., *Evaluation of residual stresses in a SOFC stack.* Journal of power sources, 2004. 131(1-2): p. 278-284.
56. Yakabe, H., et al., *Evaluation of the residual stress for anode-supported SOFCs.* Journal of Power Sources, 2004. 135(1-2): p. 9-16.
57. Fischer, W., et al., *Residual stresses in planar solid oxide fuel cells.* Journal of Power Sources, 2005. 150: p. 73-77.
58. Yakabe, H., et al., *3-D model calculation for planar SOFC.* Journal of power sources, 2001. 102(1-2): p. 144-154.
59. Selimovic, A., et al., *Steady state and transient thermal stress analysis in planar solid oxide fuel cells.* Journal of Power Sources, 2005. 145(2): p. 463-469.
60. Nakajo, A., et al., *Modeling of thermal stresses and probability of survival of tubular SOFC.* Journal of Power Sources, 2006. 158(1): p. 287-294.
61. Chen, W. and C. Nelson, *Thermal stress in bonded joints.* IBM Journal of Research and Development, 1979. 23(2): p. 179-188.

62. Radovic, M., et al., *Thermophysical properties of YSZ and Ni-YSZ as a function of temperature and porosity.* Advances in Solid Oxide Fuel Cells II: Ceramic Engineering and Science Proceedings, Cocoa Beach, Volume 27, 2009(4): p. 79.
63. *AZO Materials.* (July 29, 2013, Accessed: January 21., 2018).
64. *Kyocera Ceramics, Accessed: January 21., 2018.*
65. Pianko-Oprych, P., T. Zinko, and Z. Jaworski, *A Numerical Investigation of the Thermal Stresses of a Planar Solid Oxide Fuel Cell.* Materials, 2016. 9(10): p. 814.
66. Kakac, S., A. Pramuanjaroenkij, and X.Y. Zhou, *A review of numerical modeling of solid oxide fuel cells.* International journal of hydrogen energy, 2007. 32(7): p. 761-786.
67. Ni, M., *2D thermal-fluid modeling and parametric analysis of a planar solid oxide fuel cell.* Energy conversion and Management, 2010. 51(4): p. 714-721.
68. Vargaftik, N.B., *Handbook of physical properties of liquids and gases-pure substances and mixtures.* 1975.
69. Span, R., et al., *A reference equation of state for the thermodynamic properties of nitrogen for temperatures from 63.151 to 1000 K and pressures to 2200 MPa.* Journal of Physical and Chemical Reference Data, 2000. 29(6): p. 1361-1433.
70. Vesovic, V., et al., *The transport properties of carbon dioxide.* Journal of physical and chemical reference data, 1990. 19(3): p. 763-808.
71. Hilsenrath, J., *Tables of thermodynamic and transport properties of air, argon, carbon dioxide, carbon monoxide, hydrogen, nitrogen, oxygen, and steam*. 1960: Pergamon Press.
72. Michaelides, E.E., *NBS/NRC Steam Tables: Thermodynamic and Transport Properties and Computer Program for Vapor and Liquid States of Water in SI Units.* Nuclear Technology, 1986. 75(2): p. 232.
73. Brown, A. and M. Ashby, *Correlations for diffusion constants.* Acta Metallurgica, 1980. 28(8): p. 1085-1101.
74. Schäfer, H., *Chemical transport reactions*. 2016: Elsevier.
75. Chan, S. and Z. Xia, *Polarization effects in electrolyte/electrode-supported solid oxide fuel cells.* Journal of Applied Electrochemistry, 2002. 32(3): p. 339-347.
76. Wang, L., et al., *A parametric study of PEM fuel cell performances.* International journal of hydrogen energy, 2003. 28(11): p. 1263-1272.